Computer Aided Stability Analysis of Forklifts Utilizing the Concept of Energy Stability

By

Surinder Singh Cheema

Thesis
Presented to the University of Manitoba
in partial fulfillment of
Masters of Sciences
in
Mechanical Engineering

University of Manitoba
Winnipeg, Manitoba
Canada

0-612-76910-0

THE UNIVERSITY OF MANITOBA

FACULTY OF GRADUATE STUDIES

*****

COPYRIGHT PERMISSION PAGE

COMPUTER AIDED STABILITY ANALYSIS OF FORKLIFTS UTILIZING THE CONCEPT OF ENERGY STABILITY

BY

SURINDER SINGH CHEEMA

A Thesis/Practicum submitted to the Faculty of Graduate Studies of The University

of Manitoba in partial fulfillment of the requirements of the degree

of

MASTER OF SCIENCE

Abstract

A forklift is a common type of material handling equipment. Forklifts carry various loads at varying speed and in different types of terrains, which may result in the machines tipping over. This can cost a lot in terms of human injury and lost productivity.

The objective of this thesis is to study the effects of variable/parameters such as load, wheelbase size, speed of the vehicle and top heaviness on the stability of forklifts. A computer-based program is developed that relates these parameters/variables to the tipping over. The approach taken is to employ the concept of energy stability. The energy stability concept determines the potential overturning of the vehicle over each edge. This thesis expands the energy stability concept to also include the stability level of the forklift at variable acceleration/deceleration. The goal is to provide insight on the stability of forklifts, which may aid in an improved design for the future.

A graphic interface is also developed to interactively demonstrate the results. The software package is applied to the stability analysis of a Caterpillar DP-90 forklift. The software is capable of indicating the bounds of many variables/parameters at which the forklift operates safely. The sensitivity of the overall stability of the forklift to many of the machine variables/parameters is also studied.

Acknowledgments

I would like to thank my advisor, Dr N. Sepehri for his guidance, suggestions, encouragement and support during the completion of my thesis.

I would also like to thank all my friends for their constant support and encouragement during this study.

Last but not the least, I would like to thank my wife Ravinder and daughter Harleen. Without their patience this work could not have been completed.

Table of Contents

List of Figures

List of Tables

Chapter 1

Introduction

Industry in the last century has seen many changes. Automation has been introduced at all levels. Operations once performed by humans have now been automated, which is safer and more efficient. The focus towards efficiency has caused us to overlook the fact that most automated procedures still require human intervention. "To err is human" – but errors can lead to serious accidents. Industrial transportation of goods is one area where automation has led us to believe in secure operation. However, experience overrules technology when other predictable and unpredictable factors come into play. Forklifts are amongst the most commonly used modes of transport in today's industry. This thesis discusses stability of forklifts.

According to United States Occupational Safety and Health Administration - OSHA, there are approximately 35,000 serious and 62,000 non-serious injuries each year as a result of powered industrial equipment incidents [1]. Around 100 accidents result in death. Thousands more involve damage of products and equipment, costing the industry millions of dollars. OSHA has identified key factors that have contributed to employee accidents involved with lift trucks. Tip-overs account for approximately 25% of all the factors [1].

Proper training of the operators can reduce the accidents substantially. At the same time, there is a limit to the perfection and efficiency achievable through training, no matter how intensive it might be.

The forklift (Figure 1.1) is the most common form of material handling machinery. The primary use of this type of machinery is to safely transport goods and materials from one location to another. It eases the workload as physical labor is replaced with a machine. However, most forklift operators assume that forklifts will have similar stability to that of a road vehicle [1]. Forklifts, when compared to automobiles, are more unstable. Automobiles and trucks have a constant center of gravity. Forklifts, on the other hand, have a perpetually changing center of gravity. This nature of movement in forklifts makes them prone to instability. Factors such as top heaviness, speed of the vehicle and gradient contribute to potential tip- overs in forklifts. Additional hazards such as rough terrain make the job site even more dangerous for forklift operators.

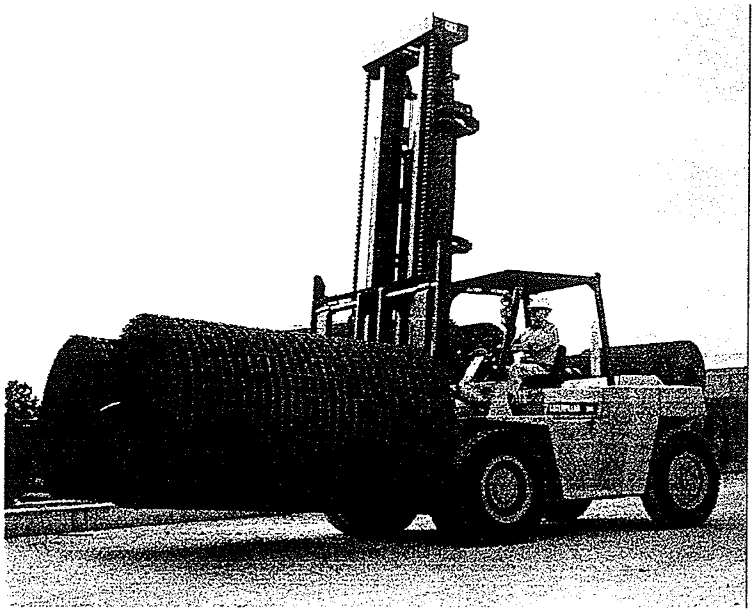

Figure 1.1: Typical forklift.

In order to improve forklift safety, the variables of instability and their impact on forklift need to be addressed. This thesis addresses this objective through development of computer software, which determines the potential instability of forklifts. The software developed could further advance the design of future forklifts.

This thesis is divided into the following chapters. Chapter 2 gives a review of the literature on the existing methods to determine the stability in mobile platforms. Chapter 3 introduces the concept of energy stability, which has been extended to determine the stability in forklifts. Chapter 4 explains the computer software development. Results obtained by computer simulations are also discussed in this chapter. The thesis is concluded in Chapter 5, which also provides suggestions for further development.

Chapter 2

Literature Review

The work on the stability of moving machines began in the late sixties, but it was related only to static stability. It was not until the early nineties that the moving nature of the machines was considered. An effort has been made to gather information about the research done on this subject and summarize it in this chapter.

This chapter first discusses the conventional methods used in industry to determine the stability of forklifts. Next, the development of methods used to determine the stability of mobile platforms will be discussed. The different methods to determine stability discussed in this chapter are:

(i) Conventional methods: Leverage method and triangle of stability method.

(ii) Advanced methods such as static stability method and zero moment point criteria.

2.1 Conventional Methods

2.1.1 Leverage Method

Consider the forklift shown in Figure 2.1. It can be considered to be a simple lever on wheels [2]. The leverage that occurs from applying force on one side of the pivot results in lifting movement on other side of the lever. The pivot point is the front axle of the forklift. If the combined center of gravity of the vehicle and the load crosses over the pivot point to the front of the body, it will result in a tip over. The factors that influence the lifting force in this case are:

- The weight of the load
- Dimensions of the load
- Weight distribution of forklift

The forklift being mobile is more complex than the case of a simple lever. There are additional dynamic forces due to the movement of the vehicle that affect its stability. Such forces are not taken into account by the simple method of leverage.

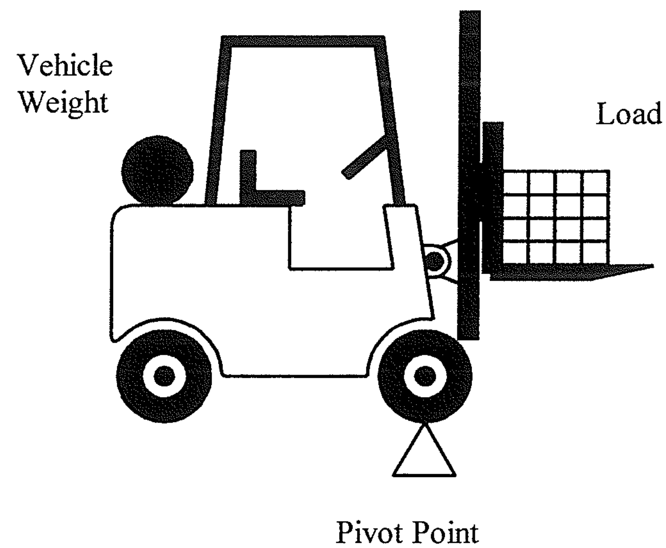

Figure 2.1: Leverage method to determine the stability of forklift.

2.1.1 Triangle of Stability Method

The instability of forklifts has also been explained with "Triangle of Stability" method [1]. A forklift has a triangle of stability area as shown in Figure 2.2. A forklift will not tip over as long as the center of gravity remains within this area. The center of gravity of a forklift can be affected by the factors such as load, top heaviness and terrain.

As in the leverage method, this method does not take into account the dynamic forces produced due to the speed of the vehicle. Furthermore it contradicts other methods of stability, one of which is that stability is maintained as long as the center of gravity remains within the supporting legs/wheels. It is also silent about the influence of height of center of gravity from the ground.

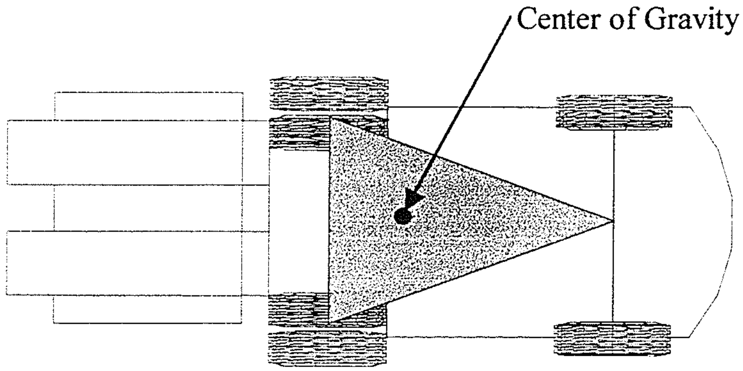

Figure 2.2: Concept of stability triangle.

2.2 Advanced Static Stability Concepts

McGee and Frank (1968) first defined the concept of static stability of a legged machine. During their study, they developed a projection method to determine the stability of a machine in movement over an even terrain.

The static stability of the legged vehicle is determined through the following definitions [3]:

(i) The *support pattern* associated with the given support state is the minimum area convex point set in the support plane such that all the leg contact points are contained.

(ii) An ideal legged locomotion machine is *statically stable* if all the legs in contact with the support plane at a given time remains in contact with that plane when all legs of machines are fixed at their location and translational and rotational velocities of resulting rigid body are simultaneously reduced to zero.

Referring to Figure 2.3, S_r and S_f are the magnitude of static stability for rear and front edges of the support boundary. The stability as defined by S_r and S_f are related to

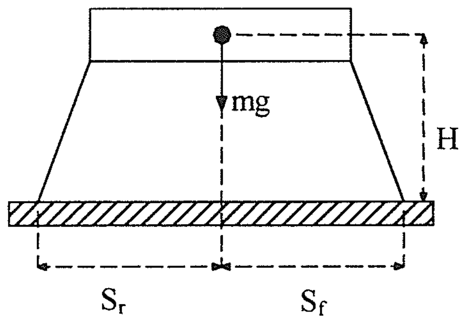

Figure 2.3: McGee and Frank's model for static stability.

moment of weight forces around the edges of the support patterns. The vehicle is on the verge of instability when the restoring moment is zero.

$$mgS_f=0 \tag{2.1}$$

In this method, the effect of height H of the center of gravity from the ground is neglected. Messuri and Klein (1985) have shown that the height of center of gravity from the ground affects the stability of the vehicle.

Song and Waldron (1987) extended the projection method to include rough terrain while working on a project on an adaptive suspension vehicle. They developed the following definitions to determine the static stability of the vehicle [4].

(i) A *support pattern* is a two-dimensional point set in a horizontal plane consisting of a convex hull of vertical projection of all foot points in support phase.

(ii) The *stability margin* is the shortest distance of vertical project of the center of gravity to the boundaries of support pattern in a horizontal plane.

Figure 2.4 shows how these definitions determine the stability of a vehicle. Consider a vehicle moving on a gradient at an angle θ with the horizontal plane. According to the

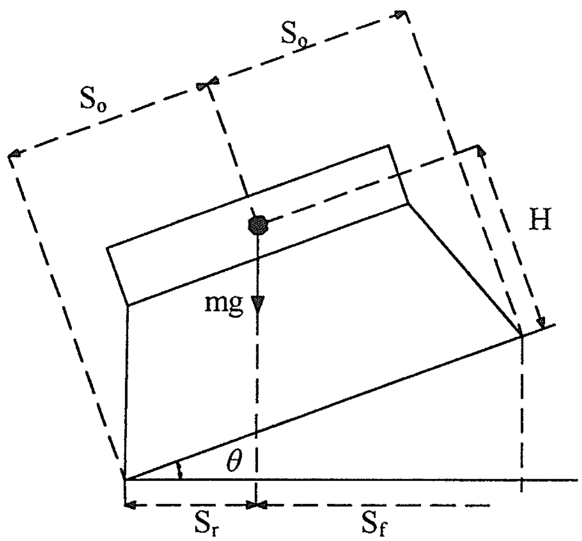

Figure 2.4: Song and Waldron's definition of static stability.

above definitions, the static stability of the front and the rear edges of the vehicle are

$$S_r = (S_0 - H\tan\theta)\cos\theta \tag{2.2}$$

$$S_f = (S_0 + H\tan\theta)\cos\theta \tag{2.3}$$

The maximum angle of inclination (θ_{max}) before the vehicle becomes unstable is determined by substituting $S_r = 0$ and solving equation (2.2)

$$\theta_{max} = tan^{-1}\left(\frac{S_o}{H}\right) \tag{2.4}$$

Although this method includes the effect of gradient on the stability, it does not include the effect of forces that are produced due to the variable speed of the machine. The other shortcoming in this method is that it does not consider the effect of top heaviness for all the cases.

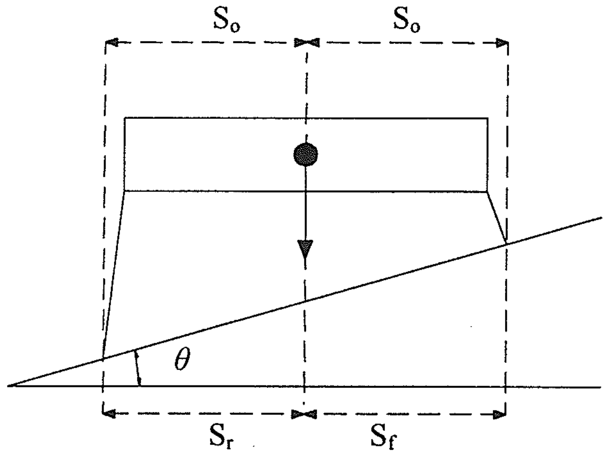

Figure 2.5: Leveled body on a gradient.

Now consider the case of a leveled body moving over a gradient as shown in Figure 2.5. According to Song and Waldron's definition of static stability, the margin of stability is maximum when $S_r = S_f = S_0$. It is clearly seen that the height H of the center of gravity is again ignored as it shows the same level of stability for the front and the rear edges. However Meseuri and Klien (1985) showed that for this condition the vehicle is subjected to tip over more easily on the rear edge rather than on the front edge.

Messuri and Klein (1985) then introduced the concept of energy stability level to determine the stability, taking into account the effect of uneven terrain. The measure of stability by this concept is developed using the following definitions [5]:

(i) The *support boundary* associated with the given support state consists of line segments which connect the tip of support feet that form the support pattern.

(ii) The *energy stability level* associated with the particular edge of the support boundary is equal to the work required to rotate the body's center of gravity, about the edge, to a position where the vertical projection of the body's center of gravity lies along the edge of the support boundary.

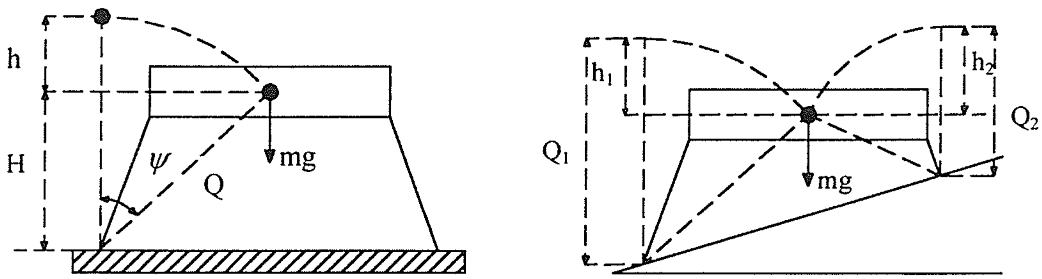

(a) (b)

Figure 2.6: Messuri and Klien definition of stability.

The application of these definitions for the vehicle moving on a horizontal plane is shown in Figure 2.6a. The energy stability level at the rear edge is

$$E = mgh = mgQ(1 - \cos\psi) \tag{2.5}$$

Here E is the energy required to bring the centre of gravity over the rear edge. Equation (2.5) shows that the effect of height of the centre of gravity is included by the relation

$$\psi = \cos^{-1}\left(\frac{H}{Q}\right) \tag{2.6}$$

Figure 2.6b shows the stability concept applied to the body moving on a gradient. It is observed that the energy required to tip over the body over the rear edge (mgh_1) is less than the energy required for the front edge (mgh_2). It is seen that the energy stability method considers the effect of the gradient on the stability of each edge of the body.

Messuri and Klien, however, neglected the effect of forces produced during movement of the body due to acceleration, deceleration or sudden stop of the vehicle. Only the weight of the body was considered in their formulation.

Ghasempoor and Sepheri (1998) improved on the concept of energy stability level and introduced a new concept of equilibrium plane, which includes the effects of destabilizing forces and moments, in addition to the weight forces, to determine the stability [6]. The shortcoming in this method is that it does not include the effect of the variable speed of the moving vehicle on the stability. As this method takes the dynamic forces, the inclination and the height of center of gravity from the ground into account, it is modified to implement on the forklift to determine its stability.

2.3 Zero Moment Point Criteria

Sugano et al. (1993) introduced the zero moment point to determine the stability of mobile manipulators. They suggested that a mobile manipulator can be considered to be a system of particles shown in Figure 2.7 [7]. The stability of the manupulator is determined based on following definitions:

(i) The *floor* is a rigid horizontal plane that will not be moved by any forces and moments (torques).

(ii) Two coordinate systems are defined. One is the *absolute Cartesian coordinate system* XYZ in which the Z-axis is the vertical direction and XOY plane is the floor. The *machine coordinate system* X'Y'Z' that is fixed to the vehicle, in which the Z' axis is the vertical direction as shown in Figure 2.7.

(iii) *Zero Moment Point (ZMP)* is a point on the floor where the resultant moment of the gravity, the inertial force and the external force is zero. If ZMP is within the stable region defined by a supporting boundary, the manupulator is stable.

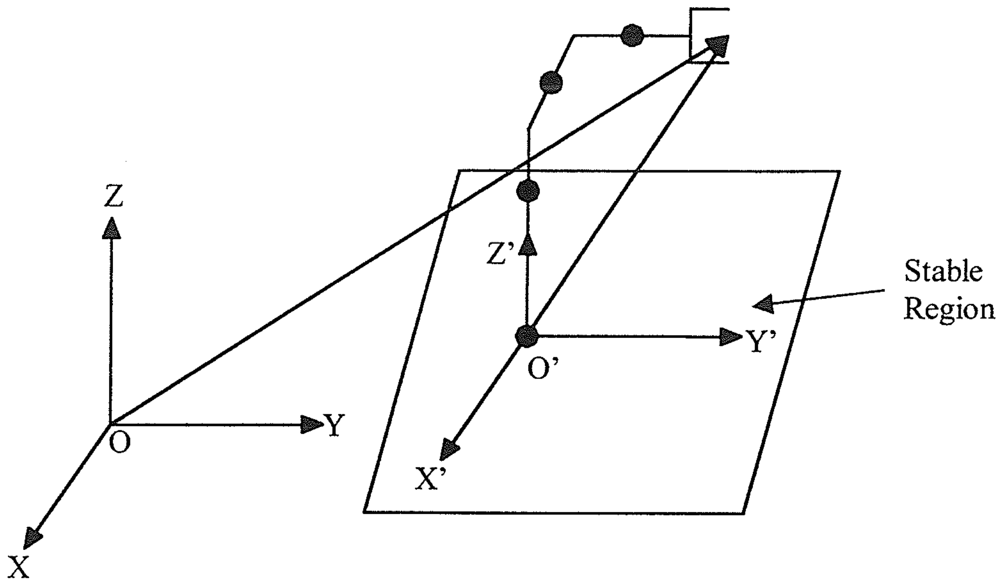

Figure 2.7 : Sugano et al's. model of mobile manupulator.

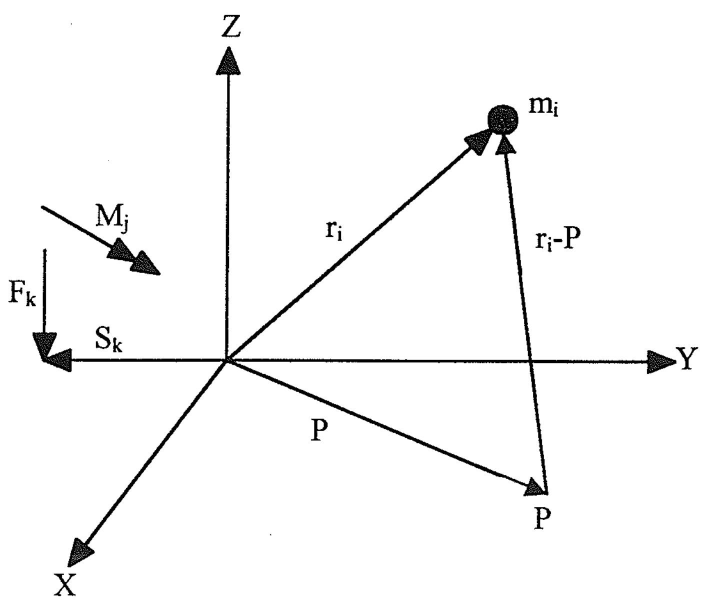

Figure 2.8: Vector description for mobile manupulator.

Referring to Figure 2.8, the equation of motion of an arbitrary point P can be given by D'Alambert's Principle [7]:

$$\sum_i m_i(r_i - P)\times\left\{\left(\frac{d^2 r_i}{dt^2}+G\right)-\frac{d^2 P}{dt^2}\right\}+T-\sum_j M_j-\sum_k (s_k - P)\times F_k = 0 \tag{2.7}$$

where,

m_i is the mass of the ith particle

$r_i = [x_i, y_i, z_i]^T$ is the position vectors of ith particle

$P = [x_p, y_p, 0]^T$ is the position of vector P

$G = [g_x, g_y, g_z]^T$ is the gravitational acceleration vector

$T = [T_x, T_y, T_z]^T$ is the resultant torque acting on point P

$M_j = [M_{xj}, M_{yj}, M_{zj}]^T$ is the external moment j

$F_k = [F_{xk}, F_{yk}, F_{zk}]^T$ is the external force k

$S_k = [x_{sk}, y_{sk}, z_{sk}]^T$ is the position vector to external force k is applied to

Solving equation 2.7, the components of ZMP can be derived as:

$$x_{ZMP} = \frac{\sum_i m_i(\ddot{z}_i + g_z)x_i - \sum_i m_i(\ddot{x}_i + g_z)z_i + \sum_j M_{yj} + \sum_k (S_{xk}F_{zk} - S_{zk}F_{xk})}{\sum_i m_i(\ddot{z}_i + g_z) - \sum_k F_{zk}} \tag{2.8}$$

$$y_{ZMP} = \frac{\sum_i m_i(\ddot{z}_i + g_z)y_i - \sum_i m_i(\ddot{y}_i + g_z)z_i + \sum_j M_{xj} + \sum_k (S_{yk}F_{zk} - S_{zk}F_{yk})}{\sum_i m_i(\ddot{z}_i + g_z) - \sum_k F_{zk}} \tag{2.9}$$

In the vehicle coordinate system, the ZMP can be found from equation:

$$[X_{ZMP}, Y_{ZMP}, 1]^T = R \times [X'_{ZMP}, Y'_{ZMP}, 1]^T \tag{2.10}$$

where, R is a 3 x 3 homogeneous transformation matrix .

The drawback with this method is that it does not take into consideration the effect of top heaviness of the vehicle to determine the stability [6]. The other shortcoming with this approach is that it neglects the manupulator moving on an inclined plane, which can be seen, from the definition of floor.

CHAPTER 3

Energy Stability Concept Applied to Forklifts

As discussed in Chapter 1, stability of forklifts is a vital area of research. Messuri and Klein (1985) developed the energy stability concept, which includes the top heaviness of the vehicle over rough terrain. Ghasempoor and Sepehri (1998) extended this concept to accommodate the effects of destabilizing forces on the stability of a vehicle carrying manupulators. This method is the most suitable for further research. Therefore, it is further developed here with specific application to forklifts.

3.1 Outline of the Concept

Consider a forklift on a gradient as shown in Figure 3.1a.The vehicle is subjected to load *mg*. The amount of work required to bring the center of gravity to the vertical plane is given by *mgh*. This Energy depends on the height *h* and not on the path followed by the center of gravity during the hypothetical rotation [5]. When the center of gravity lies in the vertical plane, the vehicle is considered to be unstable.

Now consider the forklift moving with the velocity *v* (Figure 3.1b). Let *F* be the net force produced at the center of gravity due to deceleration of the forklift. While this force is present in the direction shown, the amount of energy required to bring the vehicle to unstable condition at edge f_l would be less. Therefore, the zero moment condition will occur when the center of gravity is rotated to plane *E* (Figure 3.1c). This plane is termed as the equilibrium plane.

In order to determine the stability level of the forklift, the center of gravity of the forklift is rotated to the equilibrium plane. Considering the case shown in Figure 3.1c, the angle ϕ, which defines the equilibrium plane with respect to the vertical plane, can be obtained by equating the summation of all moments around edge f_l, i.e.

$$\sum_{f_l} M = F_t R + mgR\,sin\phi = 0 \qquad (3.1)$$

Where, F_t is the component of force tangent to the circular path. The angle, ϕ is determined by the following relation

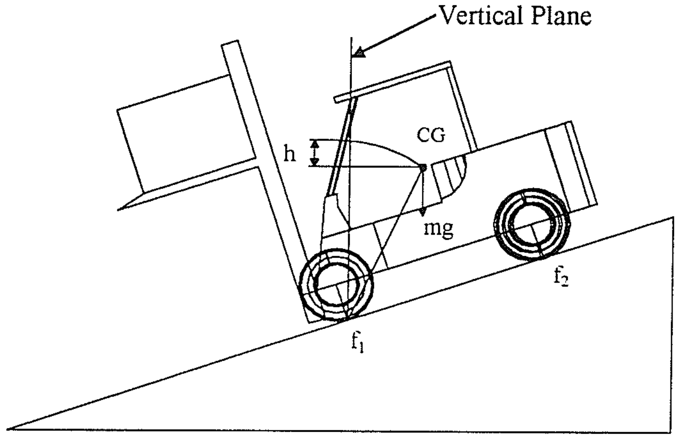

(a)

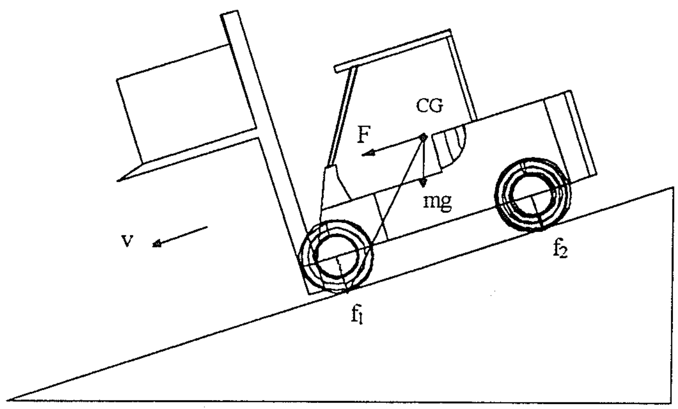

(b)

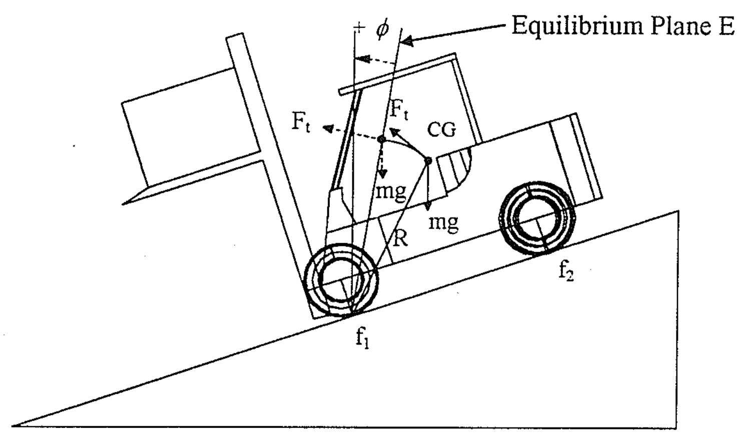

(c)

Figure 3.1: Concept of equilibrium plane.

$$\phi = -sin^{-1}\left(\frac{F_t}{mg}\right) \tag{3.2}$$

In Equation 3.2, it is assumed that the direction of force does not change during the hypothetical rotation.

In Equation 3.2 if $F_t \geq mg$, then the sum of moments about edge f_l will never be zero and therefore the angle ϕ cannot be found. In this case the vehicle would be stable.

Definitions used to determine the stability are discussed below [6]:

(i) *Equilibrium plane* associated with a particular edge of a support boundary is a plane containing the edge and with an orientation with respect to the vertical plane such that if the body is rotated around the edge until the center of gravity falls in this plane, the net moment of all present forces and moments around the edge becomes minimum in the absolute sense.

(ii) *Energy stability level* associated with a particular edge of a support boundary is equal to the work done to rotate the vehicle body (which is subjected to gravitational as well as external forces) about the edge, until the center of gravity reaches the equilibrium plane.

3.2 Formulation

The following steps are performed to determine the energy stability level of a forklift:

1. Determination of the center of gravity of the forklift.

2. Finding the equilibrium plane.

3. Calculating the work done by gravitational forces.

4. Calculating the work done by forces produced due to acceleration/deceleration.

5. Determination of the total stability level of the forklift.

3.2.1 Determining the Center of Gravity

Consider a forklift moving on an inclined plane as shown in Figure 3.2. The frame $X_GY_GZ_G$ is the global coordinate attached at the center of the rear axle of the forklift in which all the local frames are defined. $X_1Y_1Z_1$ and $X_2Y_2Z_2$ are the local frames attached at the bottom of the rear and front right tires in which the coordinates of loads m_1 and m_2 on each axle is defined. The center of gravity of the load on the fork (m_3) is defined in coordinates frame $X_3Y_3Z_3$.

To find the center of gravity of the forklift, the coordinates of the loads m_1, m_2 and m_3 are determined in the global coordinate frame $X_GY_GZ_G$.

The coordinates of load m_1 (Figure 3.2a) in frame $X_GY_GZ_G$ are determined from,

$$\begin{pmatrix} 1 & 0 & 0 & 0 \\ 0 & 1 & 0 & 0 \\ 0 & 0 & 1 & -z \\ 0 & 0 & 0 & 1 \end{pmatrix} \begin{pmatrix} x_1 \\ y_1 \\ z_1 \\ 1 \end{pmatrix} \qquad (3.3)$$

where x_1, y_1, z_1 are the coordinates of m_1 in frame $X_1Y_1Z_1$.

Similarly, the coordinates of m_2 in global coordinate system can be shown by

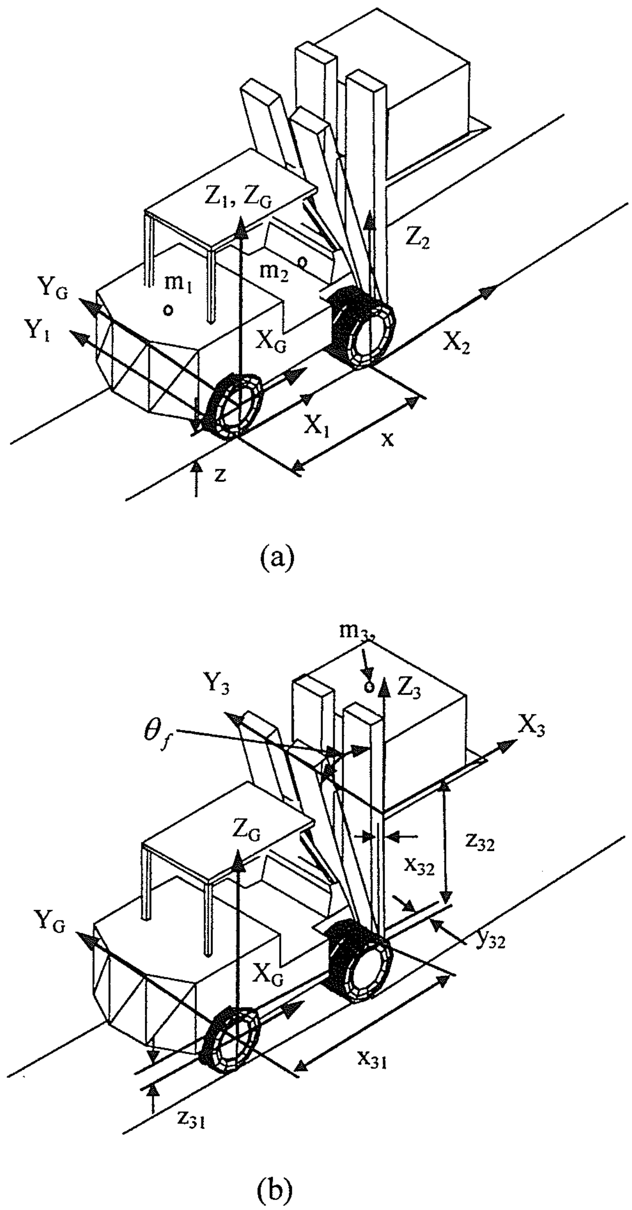

Figure 3.2: Coordinate frame of the forklift.

$$\begin{pmatrix} 1 & 0 & 0 & x \\ 0 & 1 & 0 & 0 \\ 0 & 0 & 1 & -z \\ 0 & 0 & 0 & 1 \end{pmatrix}\begin{pmatrix} x_2 \\ y_2 \\ z_2 \\ 1 \end{pmatrix} \tag{3.4}$$

where x_2, y_2, z_2 are the coordinates of m_2 in frame $X_2Y_2Z_2$.

Referring to Figure 3.2b the coordinates of fork load (m_3) in coordinate frame $X_GY_GZ_G$ are

$$\begin{pmatrix} cos\theta_f & 0 & sin\theta_f & x_{31}+x_{32}cos\theta_f+z_{32}sin\theta_f \\ 0 & 1 & 0 & y_{32} \\ -sin\theta_f & 0 & cos\theta_f & z_{31}+z_{32}\cos\theta_f-x_{32}\sin\theta_f \\ 0 & 0 & 0 & 1 \end{pmatrix}\begin{pmatrix} x_3 \\ y_3 \\ z_3 \\ 1 \end{pmatrix} \tag{3.5}$$

where θ_f is the angle that the fork makes with the vertical plane when the forklift is on a horizontal plane and x_3, y_3, z_3 are the coordinates of m_3 in frame $X_3Y_3Z_3$.
Solving for the equation 3.3, 3.4 and 3.5, the center of gravity of the forklift is found from the equation:

$$\vec{R}_{cg} = \begin{bmatrix} x_{cg} \\ y_{cg} \\ z_{cg} \end{bmatrix} = \frac{\sum_{i=1}^{3} m_i s_i}{\sum_{i=1}^{3} m_i} \tag{3.6}$$

where $\vec{R}_{cg}$ is the position vector of the center of gravity of the forklift defined in global frame and $\vec{s}_i$ is the position vector of m_i defined in global frame.

Figure 3.3 shows the coordinate system attached to the center of gravity of the forklift. XYZ is the machine coordinate system and this frame moves with the forklift and Z is always in the direction perpendicular to the terrain. It is defined as machine frame. The forces produced due to variable velocity of the vehicle are calculated in this frame.

Frame $\overline{X}\,\overline{Y}\,\overline{Z}$ is defined as the gravity frame. $\overline{Z}$ is in the direction opposite to the gravitational acceleration. The machine frame and gravity frame change as the center of gravity of the vehicle changes. These two frames coincide with each other when the vehicle is moving on a horizontal frame. These two frames are separated by two rotational angles for roll ϕ_x and pitch ϕ_y.

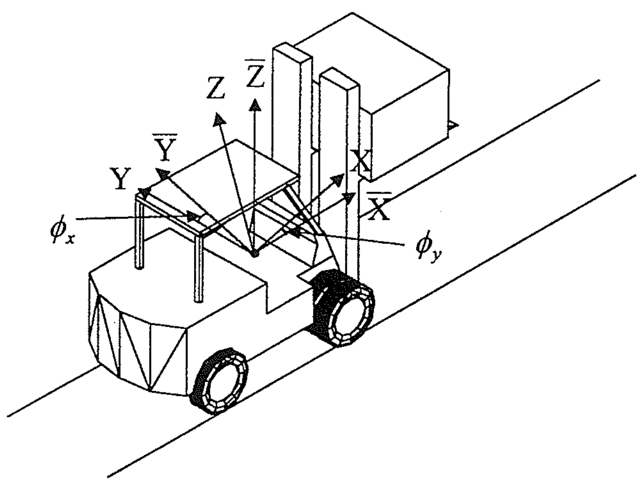

Figure 3.3: Coordinate systems for forklift.

3.2.2 Determining the Equilibrium Plane

The vectors to determine the equilibrium plane are shown in Figure 3.4. The gravity and machine coordinates have the same origin at the center of gravity of the forklift. The load and forces produced due to variable velocity are acting on the CG of the machine. The contact points of the edge where the forklift is subject to tip over are f_1 and f_2. So the unit vector $\tilde{b}$ in the direction connecting f_1 and f_2 in the machine coordinate system is

$$\tilde{b} = \frac{(\vec{f}_2 - \vec{f}_1)}{|\vec{f}_2 - \vec{f}_1|} \tag{3.7}$$

where vectors $\vec{f}_1$ and $\vec{f}_2$ define the position of contact points f_1 and f_2 in the XYZ frame. $\vec{R}$ is vector orthogonal to vector $\overline{f_1 f_2}$ such that,

$$\vec{R} \bullet \tilde{b} = 0 \tag{3.8}$$

Vector $\overline{f_1 C}$ connecting point f_1 to C can be defined as

$$\overline{f_1 C} = \lambda \tilde{b} \tag{3.9}$$

where λ is the length of vector $\overline{f_1 C}$.

Knowing that

$$\vec{f} + \lambda \tilde{b} = -\vec{R} \tag{3.10}$$

From Equation (3.8)

$$\left(\lambda \tilde{b} + \vec{f}_1\right) \bullet \tilde{b} = -\vec{R} \bullet \tilde{b} = 0 \tag{3.11}$$

Therefore λ can be calculated from Equation (3.11)

$$\lambda = -\vec{f}_1 \bullet \tilde{b} \tag{3.12}$$

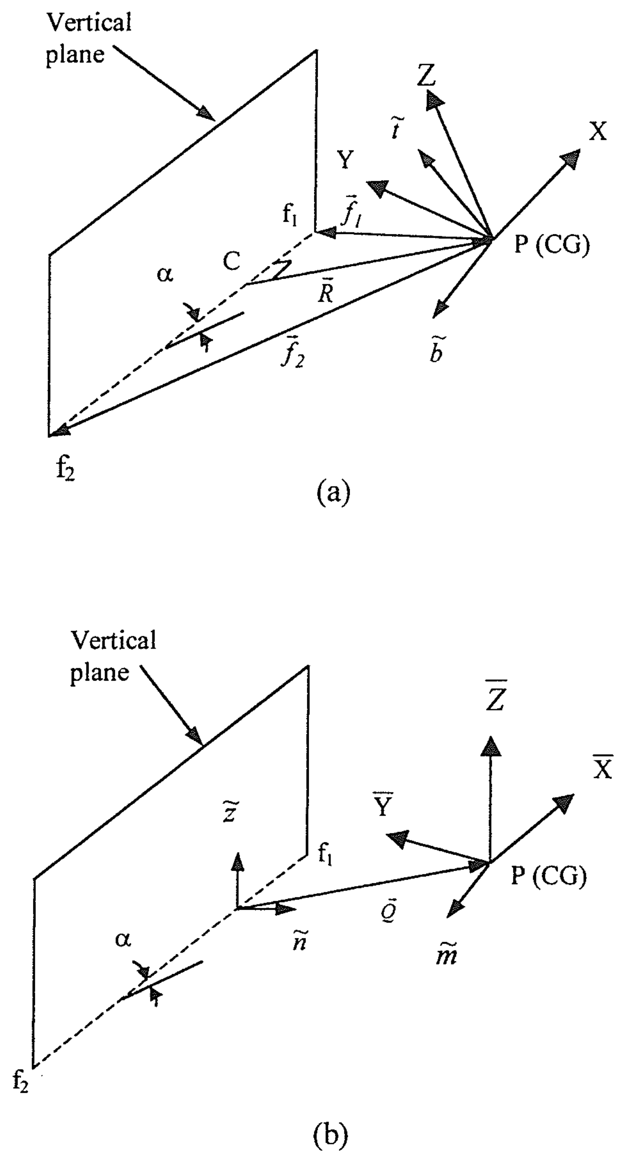

Figure 3.4: Vector description to determine equilibrium plane.

(a) In machine frame. (b) In gravity frame.

As $b^2 = 1$, vector $\vec{R}$ can be calculated by substituting λ in Equation 3.11. Thus,

$$\vec{R} = \left(\vec{f}_1 \bullet \tilde{b}\right)\tilde{b} - \vec{f}_1 \tag{3.13}$$

Unit vector $\tilde{t}$ perpendicular to plane PCf_1 is determined by the following equation

$$\tilde{t} = \tilde{b} \times \frac{\vec{R}}{|\vec{R}|} \tag{3.14}$$

Similarly, referring to Figure 3.4b vector $\vec{Q}$ is orthogonal to vector $\overline{f_1 f_2}$ and connected to the center of gravity (CG) of the vehicle.

Unit vector $\tilde{m}$ in the $\overline{X}\ \overline{Y}\ \overline{Z}$ frame connecting f_1 and f_2 can be given by

$$\tilde{m} = \frac{(\vec{f}_2 - \vec{f}_1)}{|\vec{f}_2 - \vec{f}_1|} \tag{3.15}$$

Vector $\vec{Q}$ can be found from the equation

$$\vec{Q} = (\vec{f}_1 \bullet \tilde{m})\tilde{m} - \vec{f}_1 \tag{3.16}$$

Two unit vectors are further defined in the $\overline{X}\ \overline{Y}\ \overline{Z}$ frame. $\tilde{z}$ is the unit vector in the direction of $\overline{Z}$, and unit vector $\tilde{n}$ which is perpendicular to the vertical plane and is defined as

$$\tilde{n} = \frac{\tilde{z} \times \tilde{m}}{|\tilde{z} \times \tilde{m}|} \tag{3.17}$$

According to the definition, equilibrium plane is the plane containing the support boundary edge f_1f_2 and center of gravity with an orientation such that the summation of all moments around the boundary edge is minimum. Equilibrium plane is at an angle ϕ from the vertical plane as shown in Figure 3.5.

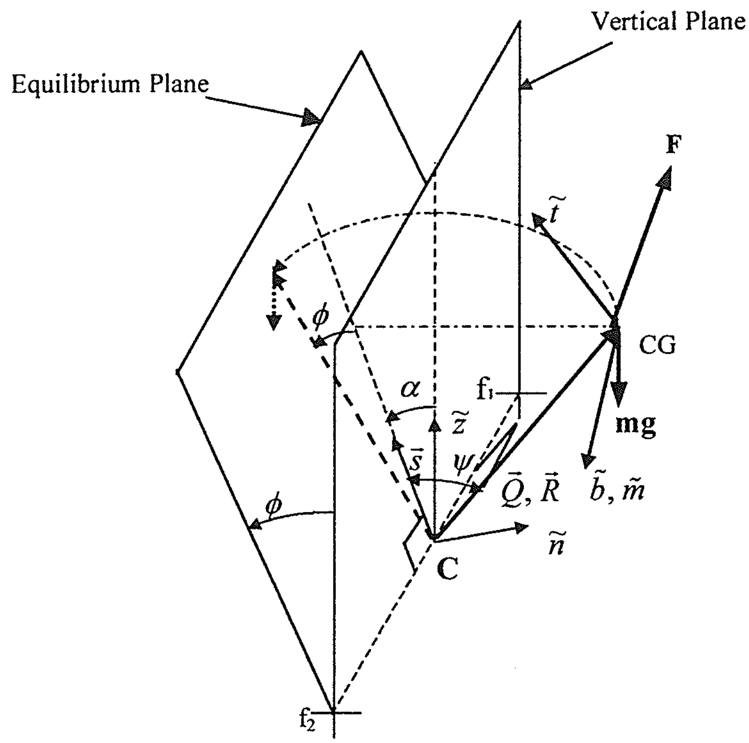

Figure 3.5: Equilibrium plane.

According to the definition of equilibrium plane, the following relation holds,

$$\sum_{around f_1 f_2} M = (\vec{F} \bullet \tilde{t}) |\vec{R}| + mg |\vec{Q}| \cos\alpha \cos\phi = 0 \qquad (3.18)$$

where F is the force produced due to acceleration/deceleration of the forklift.

ϕ can then be found from equation (3.18) as

$$\phi = \begin{cases} -\sin^{-1} \dfrac{\vec{F} \bullet \tilde{t})\,|\,\vec{R}\,|}{mg\,|\,\bar{Q}\,|\cos\alpha} \; for\,|\,(\vec{F} \bullet \tilde{t})\,|\,\vec{R}\,\|\leq mg\,|\,\bar{Q}\cos\alpha \\ 90°\, for\,|\,(\vec{F} \bullet \tilde{t})\,|\,\vec{R}\,\|\geq mg\,|\,\bar{Q}\cos\alpha \end{cases} \tag{3.19}$$

where the numerator is defined in XYZ frame and the denominator is defined in $\overline{\mathrm{X}}\,\overline{\mathrm{Y}}\,\overline{\mathrm{Z}}$ frame.

The angle α in equation 3.19, which the support boundary edge makes with the horizontal plane, can be given by,

$$\alpha = \cos^{-1}\left(\tilde{z} \bullet \frac{\vec{s}}{|\,\vec{s}\,|} \right) \tag{3.20}$$

where vector $\vec{s}$ is perpendicular to line f_1f_2 and is defined as

$$\vec{s} = \tilde{m} \times \vec{n} \tag{3.21}$$

When the vehicle is moving at a constant velocity, i.e. acceleration of the vehicle is zero, then the vertical plane coincides with the equilibrium plane and angle ϕ is zero as the force $\vec{F}$=0.

3.2.3 Work Done by Gravitational Force

According to the definition of energy stability, work done by the gravitational force to bring the center of gravity of the vehicle to the equilibrium plane is given by (Figure 3.6),

$$W_1 = -mgh \tag{3.22}$$

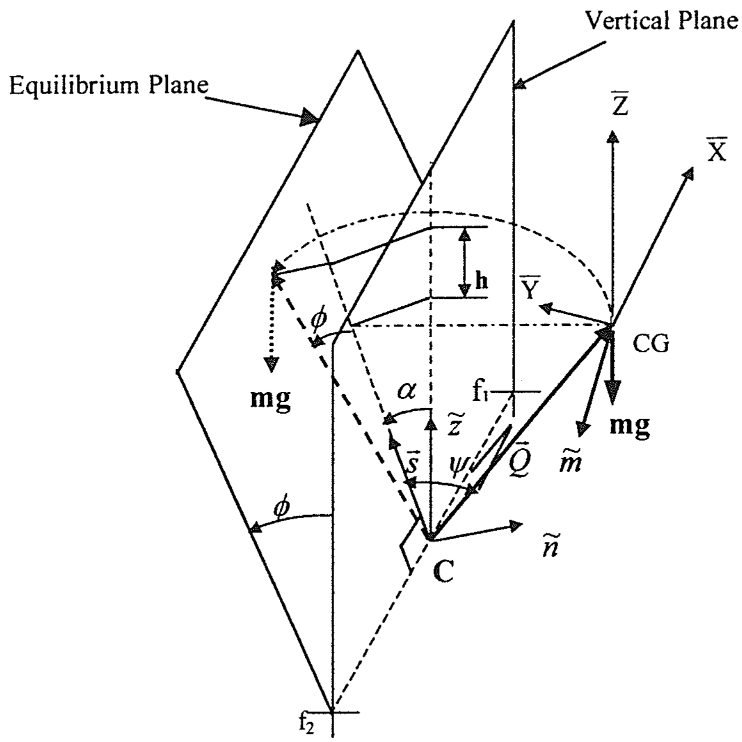

Figure 3.6: Work done by gravitational force.

Where h can be calculated from the equation

$$h = |\vec{Q}|(\cos\phi - \cos\psi)\cos\alpha \qquad (3.23)$$

where ψ is the angle between vertical plane and $\vec{Q}$ is

$$\psi = \cos^{-1}\left(\frac{\vec{Q}}{|\vec{Q}|} \bullet \frac{\vec{s}}{|\vec{s}|}\right) \qquad (3.24)$$

3.2.4 Work Done By Other Forces

This part calculates the work done by the destabilizing force produced due to acceleration/deceleration of the vehicle. According to D'Alemberts principle, the force

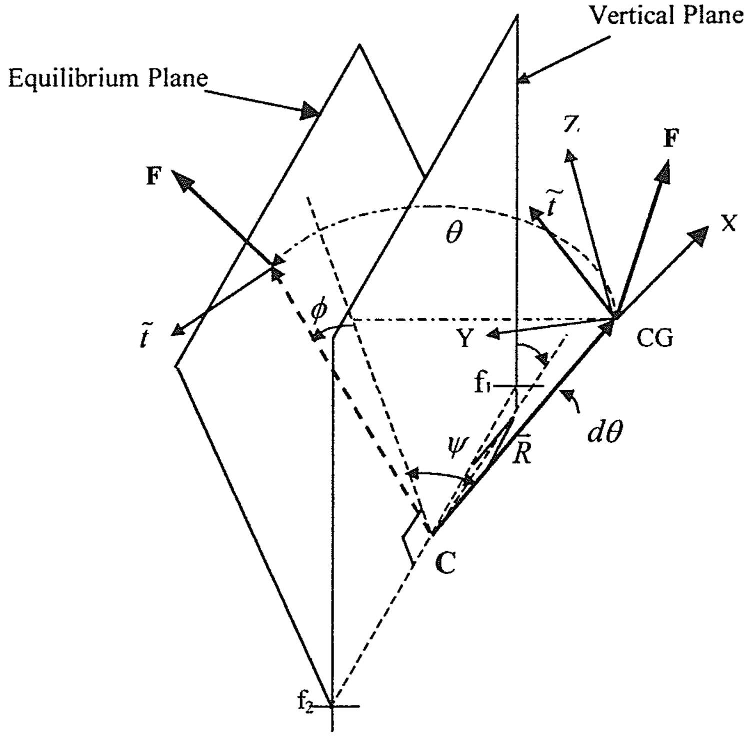

Figure 3.7: Work done by other forces.

$\vec{F}$ produced due to variable velocity of the forklift can be stated by the following equation:

$$\vec{F} = -m\vec{a} \tag{3.25}$$

where m is the total mass of the forklift and $\vec{a}$ is the acceleration of the center of gravity of the forklift. The work done by the destabilizing force during hypothetical rotation of the center of gravity of the forklift over the support boundary edge is shown in Figure 3.7 and is given by

$$W_2 = \int (\vec{F} \bullet \tilde{t})ds \tag{3.26}$$

where $ds = |\vec{R}|\, d\theta$

These vectors are defined in XYZ frame. During the hypothetical rotation of the forklift over edge f_1f_2, the direction of force $\vec{F}$ does not change relative to machine coordinates.

Therefore $(\vec{F} \bullet \tilde{t})$ remain constant, and

$$W_2 = (\vec{F} \bullet \tilde{t})\,|\,\vec{R}\,|\int d\theta \qquad (3.27)$$

$$W_2 = (\vec{F} \bullet \tilde{t})\,|\,\vec{R}\,|\,\theta \qquad (3.28)$$

where $\theta = \psi + \phi$

3.2.5 Total Energy Stability Level

According to the definition, the energy stability level of edge f_1f_2 of the support boundary is

$$\text{Energy Stability Level}_{f_1f_2} = -(W_1 + W_2) \qquad (3.29)$$

3.2.6 Special Case Of Abrupt Stop

Now consider the forklift moving with the velocity $\vec{v}$, is brought to an abrupt stop. The angular velocity around f_1f_2 due to this velocity is given by

$$\vec{Q} \times m\vec{v} = I_{f_1f_2}\vec{\omega}_{f_1f_2} \qquad (3.30)$$

where $I_{f_1f_2}$ is the total inertia of the forklift.

If the angular velocity promotes instability $(\vec{\omega}_{f_1f_2} \bullet \tilde{m} > 0)$, then the energy stability level of the forklift is

$$\text{Energy Stability Level}_{f_1f_2} = -W_1 - \frac{1}{2} I_{f_1f_2} \omega_{f_1f_2}^2 \tag{3.31}$$

Equations (3.29) and (3.31) determine the energy stability level for each edge at any instance for the case of acceleration/deceleration and sudden stop.

Chapter 4

Implementation and Results

Industry relies on experienced drivers for the safe operation of forklifts. However, safety can also be increased if we can anticipate when the forklift will be unstable. By predefining the variables such as load on the fork, height of the fork from the ground, speed and direction of the vehicle with respect to dimensions of the vehicle, the tipping over of the machine can be predicted. This procedure is complex but can be done accurately and precisely with the help of computers. A software program was designed to take all available variables/parameters into consideration and make accurate predictions of the accident.

4.1 Software Development

The programming language used in developing the software is Visual C++. It is one of the most efficient application development tools and is widely used in the development of software used in industry [8]. It has a comprehensive set of features that support the development and implementation of various functional requirements. Another application called Open GL is used to display the graphics of this software due to its good three-dimensional capabilities. Open GL is independent of the operating system and the hardware platform, making it an independent graphics library designed to be easily portable and rapidly executable. The software is divided into three modules; (i) module of accepting the system parameters, (ii) module for calculating the stability level and (iii) graphical display module.

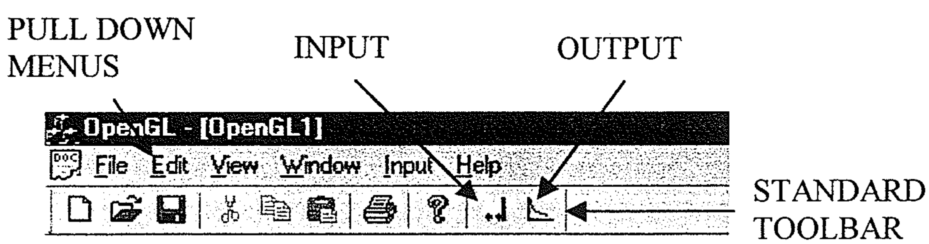

Figure 4.1: Snap shot of control box.

As the software executes the screen showing the toolbars, clicking on the Input icon (Figure 4.1) will give a dialog box as shown in Figure 4.2. It contains various parameters with fields with editable default values.

The variable dialog box can also be viewed from the pull down menus. Select 'Input' on the pull down menu and then 'Dimensions' (Figure 4.1). Other method to view the variable dialog box is by clicking on the yellow forklift icon in the standard toolbar.

The variable dialog box is partitioned into seven segments (refer to Figure 4.2):

1. Dimensions of forklift in meter.
2. Angles in degree.
3. Load in kg.
4. Dimensions of load in meter.
5. Dimensions of fork in meter
6. Rotation point from front axle in meter.
7. Speed in km/h.

The variables of the forklift are shown in Figure 4.3. θ_v is the turning angle of the forklift. θ_f is the angle that the fork makes with the vertical plane while the forklift is on a horizontal plane. The dimensions of the rotation point of the fork are with respect to the center of the front axle, the horizontal distance (Rx) and the vertical distance (Rz). Other inputs are the load on each axle and the fork, dimensions of the load, fork height and speed of the vehicle. Other inputs are the angles for pitch and roll, i.e, ϕ_x and ϕ_y in Section 3.2.1.

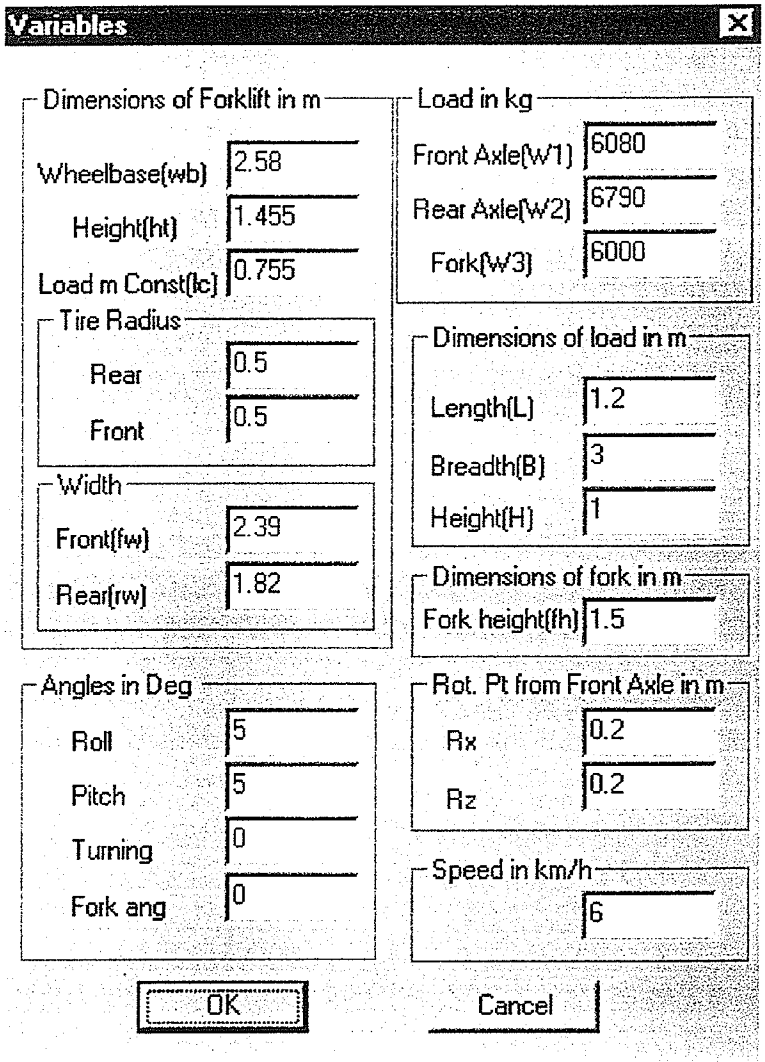

Figure 4.2 User interface for defining forklift parameters.

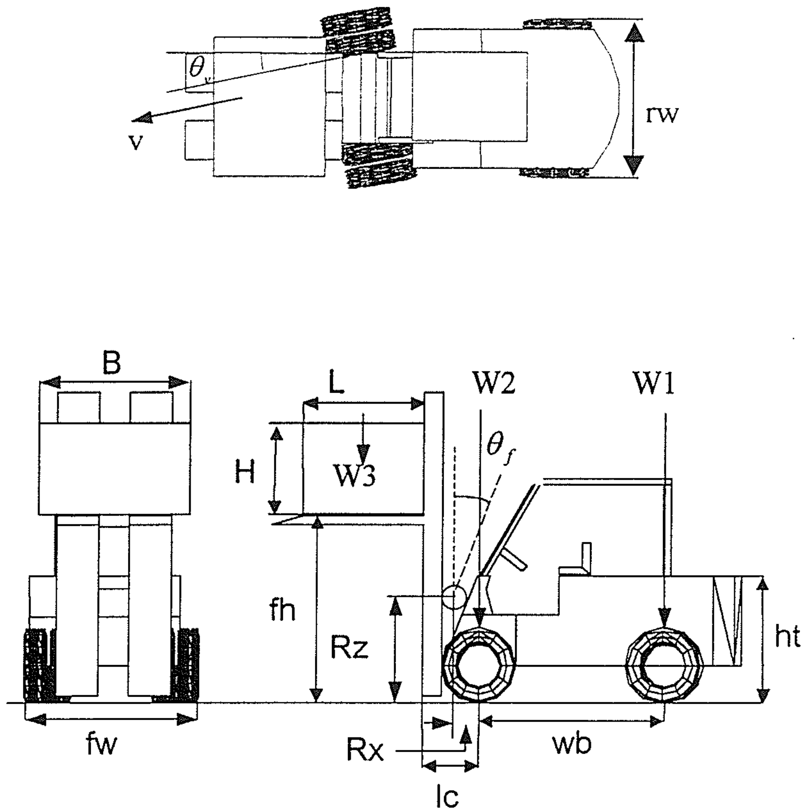

Figure 4.3: Variables of forklift.

Output can be extracted in different forms. The available outputs are shown in Figure 4.4.

They are divided into three modules:

1. Variables.

2. Plots for energy stability level.

3. Acceleration/Deceleration.

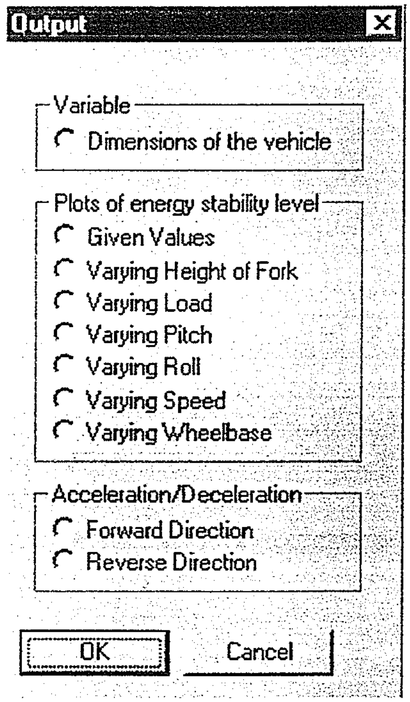

Figure 4.4: User interface for plotting the desired outputs.

First module "Variables" shows the dimensions of the forklift on the screen. Second module is "Plots of energy stability level" which show the results of particular case when the vehicle is brought to a sudden stop. This depends on the input variables. The last module "Acceleration/Deceleration" depicts the results for the stability of each edge of the forklift when it is accelerated/decelerated. For the front and rear edges, the software is capable of calculating the energy stability level either at the axles of the tires, or at the contact point of the tires with the ground.

The energy stability concept discussed in Section 3.2 is used to develop the software to determine the stability level of each edge of the boundary of the forklift. After determining the center of gravity of the forklift, the energy stability level of each edge of the forklift is the function of:

$$Energy\ Stability\ Level = F(f_1, f_2, \phi_x, \phi_y, m, \vec{v})$$

where f_1 and f_2 are the coordinates of feet contact point with respect to the center of gravity of the vehicle. ϕ_x is the roll angle of the vehicle base with the horizontal plane in degrees. ϕ_y is the pitch angle of the vehicle base with the horizontal plane in degrees. m is the total mass of the forklift and the load on the fork in kg. $\vec{v}$ is the velocity of the forklift in km/h. The flow chart of the algorithm to determine the energy stability level is shown in Figure 4.5.

Energy Stability is calculated for each edge of the support boundary of the forklift. After calculating the energy stability level for each edge of the support boundary of the forklift, the results are plotted on the screen. Table 4.1 shows the minimum and maximum limits for all variables in order to calculate the stability level of the forklift.

A typical output of the computer software for variable load on the fork is shown in Figure 4.6. The four plots in the corners of the screen show the stability level of each edge of the vehicle. The red lines represent the stability when the vehicle is brought to an abrupt stop. The green lines indicate the stability level of the vehicle while the machine is moving at a constant speed.

4.2 Case Studies

The software was used to investigate the effects of different variables and parameters on the stability of a Caterpillar DP-90 forklift. The dimensions of the forklift are shown in the appendix. To illustrate the execution of the software, a hypothetical situation is considered. The dimensions of the load on the fork and other variables used for the case study are shown in Table 4.2.

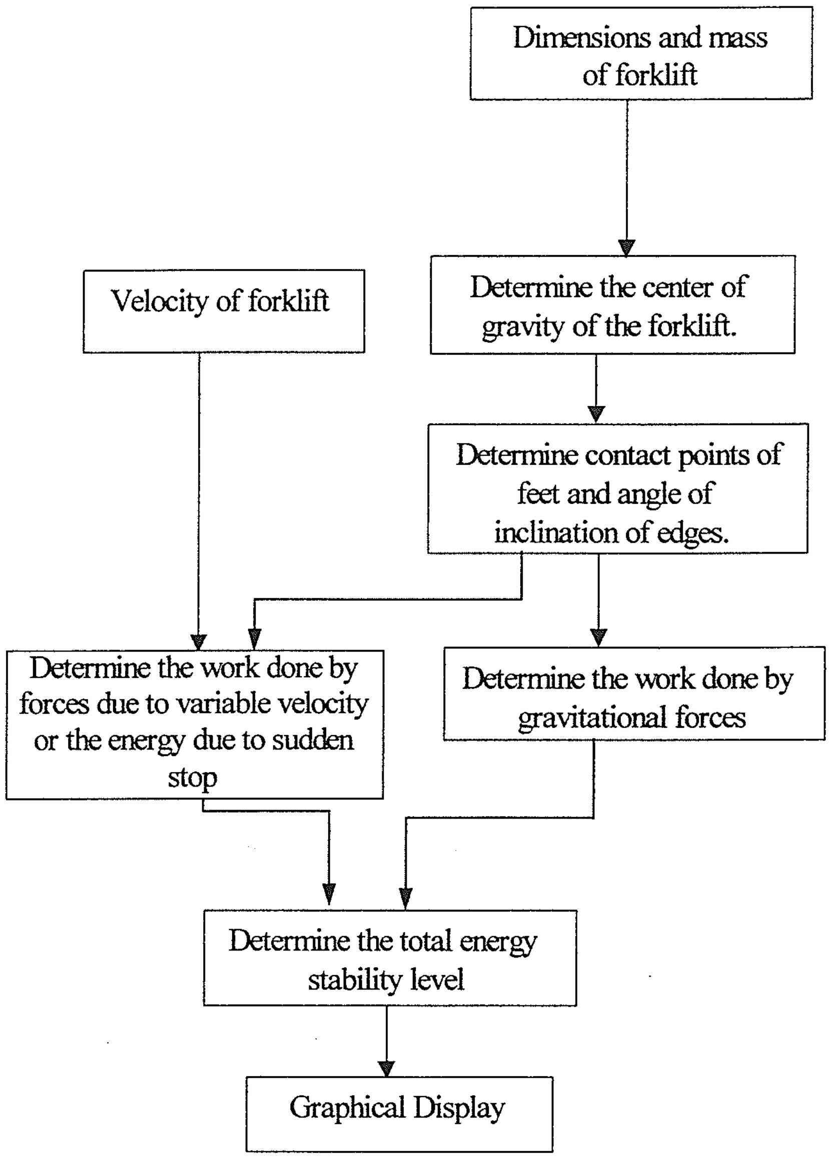

Figure 4.5: Flow chart to determine stability of forklift.

Table 4.1: Limits of variables.

Variable	Minimum	Maximum
Height	**0.0 m**	**4.0 m**
Load	**0**	**10,000 kg**
Pitch	**-15°**	**15°**
Roll	**-15°**	**15°**
Velocity	**-15 km/h**	**15 km/h**
Wheel base	**0.5 m**	**3.5 m**

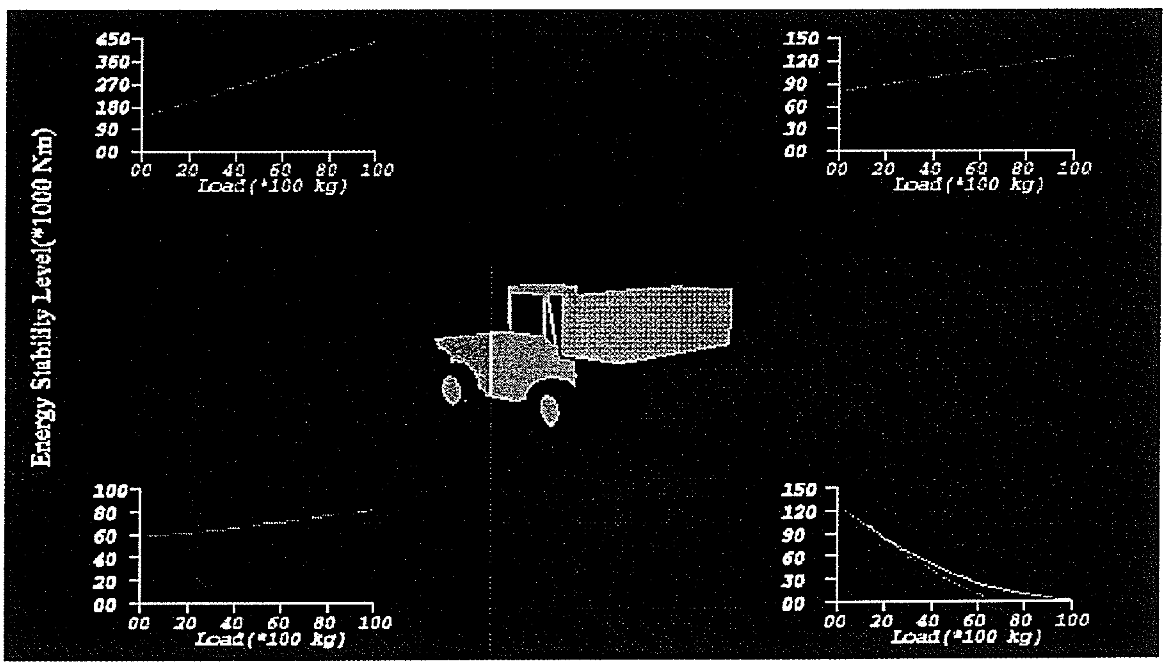

Figure 4.6: Graphical results of software.

Table 4.2: Default values of variables used for case studies.

Variable	L	B	H	W3	Speed
Value	1.2 m	3 m	1 m	5,000 kg	6 km/h
Variable	Roll angle	Pitch angle	Turning angle	Fork angle	Fork height
Value	0°	0°	0°	0°	1.5 m

4.2.1 Effect of Varying Load

The energy stability level of each edge of the forklift for variable loads is shown in Figure 4.7. The load is varied from 0 to 10,000 kg at the height of 1.5 meters of the fork from the ground. Figure 4.7a shows the energy stability level of the vehicle while it is at a constant speed of 6 km/h. Figure 4.7b represents the stability level of the forklift when it is brought to an abrupt stop from 6 km/h.

The results show that with an increase in load on the fork, the energy stability level of edge 1 decreases whereas the stability level of the other edges increases. It is observed that when the vehicle is brought to a sudden stop from 6 km/h, it is subjected to tipping over on edge 1 at loads above 5,800 kg. When the vehicle is moving at a constant speed, the vehicle is stable even at the fork load of 10,000 kg. The maximum recommended load on the fork of a Caterpillar DP-90 forklift is 9,000 kg, with its center of gravity at 0.6 meters from load moment constant.

It is observed that the stability level of edges 2, 3 and 4 is the same for both sudden stop and constant velocity. The stability level of edge 1 at zero load is approximately the same for both cases. As the load on the fork is increased, the difference between the two

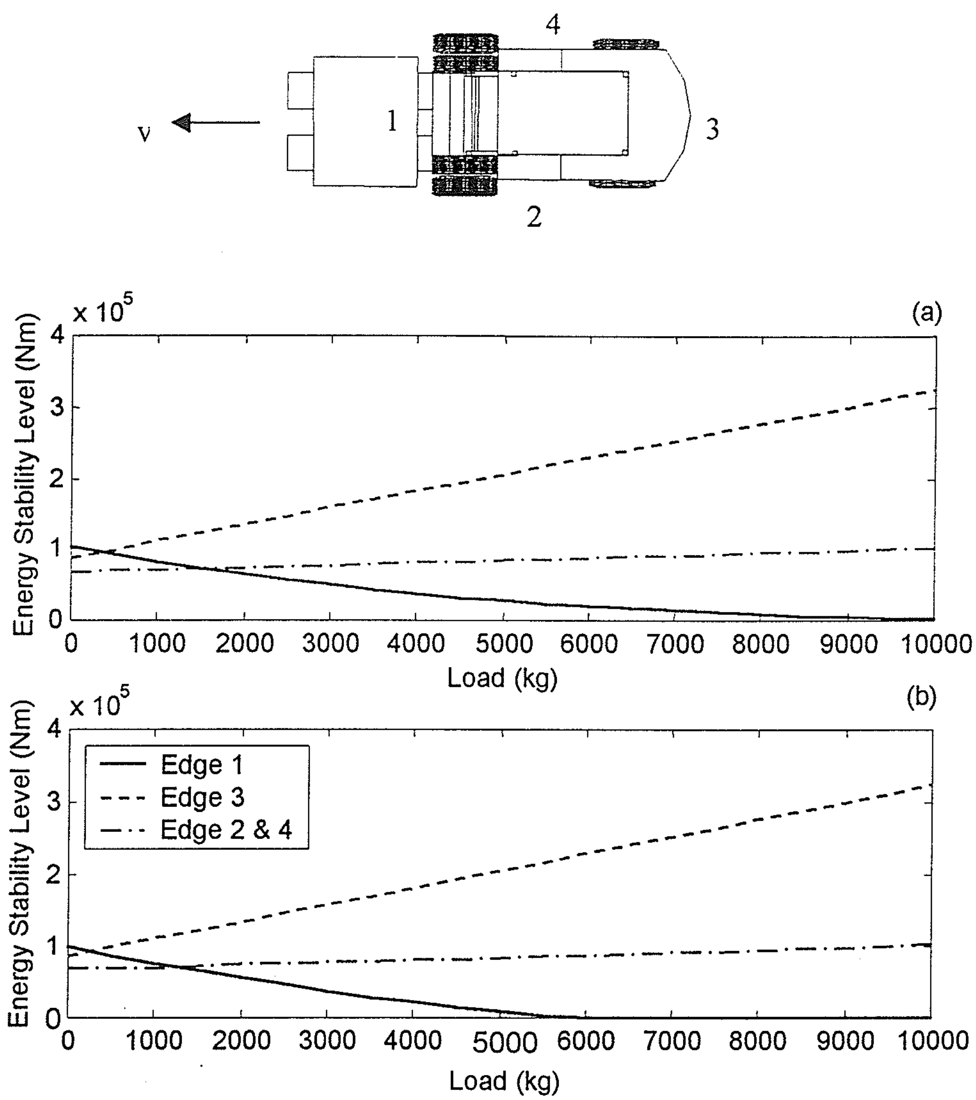

Figure 4.7: Energy stability level at varying load:

(a) Constant velocity; (b) Abrupt stop.

curves become more evident. It is observed that the difference in energy stability levels for the fork load of 0 and 500 kg is 11818 Nm and for the fork load of 5,000 and 5,500 the difference is 5732 Nm. Therefore, the results show that with the increase in load on the fork, the difference in the energy stability levels of two consecutive loads decreases. To the contrary, for edges 2,3 and 4 an increase in load results in an increase in the difference in the stability level of two consecutive loads.

4.2.2 Effect of Varying Gradient

Effect of gradient is investigated with this software. Forklift stability, when it is operating on a gradient, is shown in Figures 4.8 and 4.9. The software was executed to determine the effect of pitch and roll (ϕ_y and ϕ_x in Section 3.2) on the stability of the forklift. The energy stability level for both the cases were observed from the inclination angle of $-15\ ^\circ$ to $15\ ^\circ$. For each case the other angle of inclination was $0\ ^\circ$.

Figure 4.8 shows that with the increase in the angle of inclination (ϕ_y), the stability level of edge 1 decreases dramatically. The stability of edge 3 increases with the increase in the angle of inclination. Referring to Figure 4.8b, at an inclination angle of above 4° the energy stability level for side 1 is zero, which means that the vehicle is on the verge of instability after 4° if it is brought to a sudden stop from the speed of 6km/h.

Figure 4.9 shows that there is an increase in stability of edge 2 and a drastic decrease in the stability of edge 4 with the increase in roll (ϕ_x in Section 3.2). The stability level for each of these two edges is the same at the angle of 0°, which is expected. The stability levels of edges 1 and 3 slightly increase when the angle of inclination is increased from -15° to 0° and decreases when the inclination angle changes from 0 to 15°.

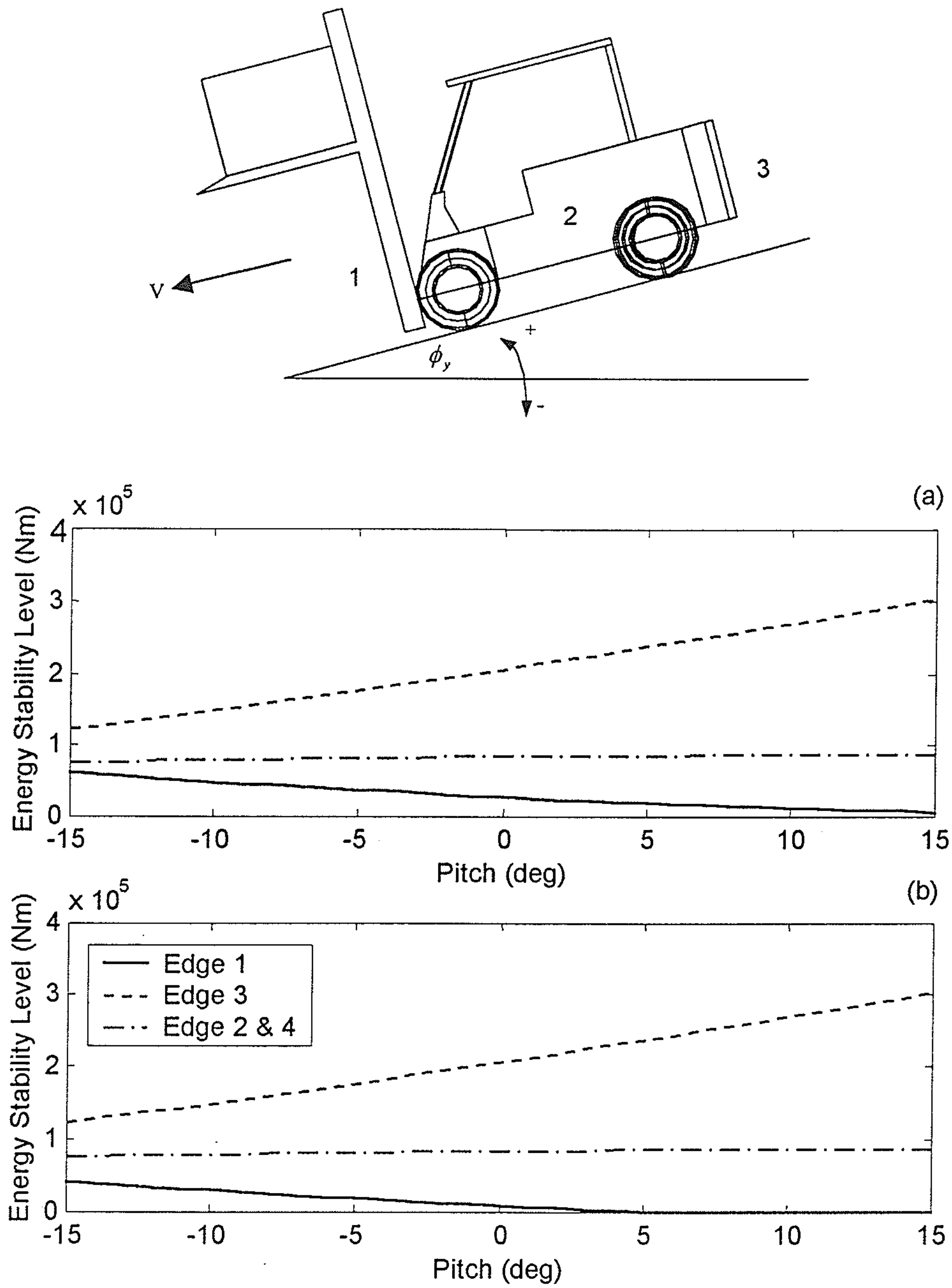

Figure 4.8: Energy stability level at varying pitch:

(a) Constant velocity; (b) Abrupt stop.

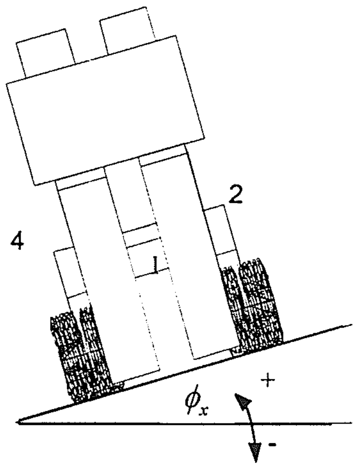

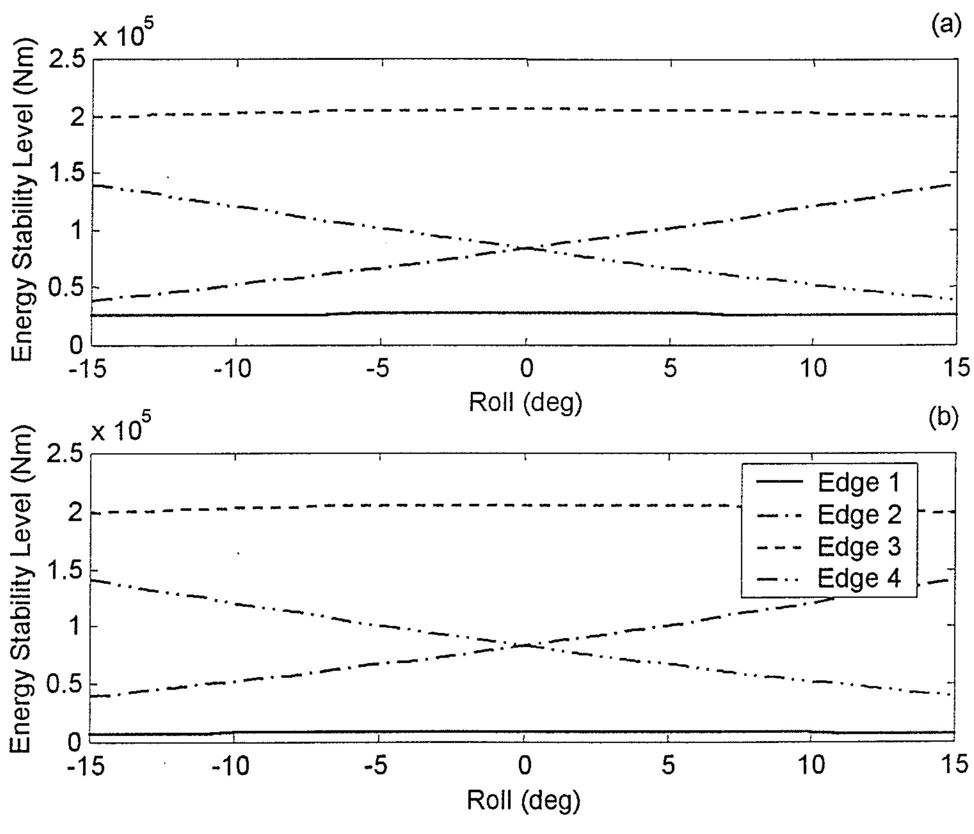

Figure 4.9: Energy stability level at varying roll:

(a) Constant velocity; (b) Abrupt stop.

4.2.3 Effect of Top Heaviness

The effect of height of fork from the ground level was also studied with this software. Figure 4.10 shows the forklift stability for variable heights of the fork. Figure 4.10a represents the stability level when the vehicle is moving at a constant speed and 4.10b represents the stability level when the vehicle is brought to an abrupt stop from 6 km/h (see Table 4.2). The graphs show that with an increase in the height of the fork, the stability of each edge of the forklift decreases. Figure 4.10 also shows that the forklift is susceptible to tipping over when the fork height is greater than 2.6m from the ground in a sudden stop condition. It is however safe up to a height of 4 m when it is moving at a constant speed.

The results show the difference in the energy stability level for the vehicle moving with the fork at ground level and at 1.6m from the ground. Under these specified conditions the difference is 19,520 Nm when the forklift is brought to an abrupt stop. This represents a 72% drop in the energy stability level. It has been observed that for the same dimensions of the load and speed, the load on the fork can increase from 5,000 kg at 1.6 m to 6,600 kg at ground level. That is an increase of 1,600 kg to bring the vehicle to the same stability level as at 1.6 meters for the case on an abrupt stop. If the height of the fork is dropped from 1.6 m to 0.4 m, the load on the fork can be increased by as much as 300 kg to bring the vehicles stability level to same condition as 1.6 m.

For the case of constant velocity, if the height is dropped from 1.6 m to ground level, the energy stability level will be the same if the load on the fork is increased from 5,000 kg to 6,500 kg. The results show that if the height of the fork is dropped from 4.0 m to 1.6 meters, the load on the fork can be increased by up to 1,350 kg. If the height of the fork is further decreased to ground level, the load on the fork can be increased by 2,700 kg (from 5,000 kg to 7,700 kg) without effecting the stability of the forklift.

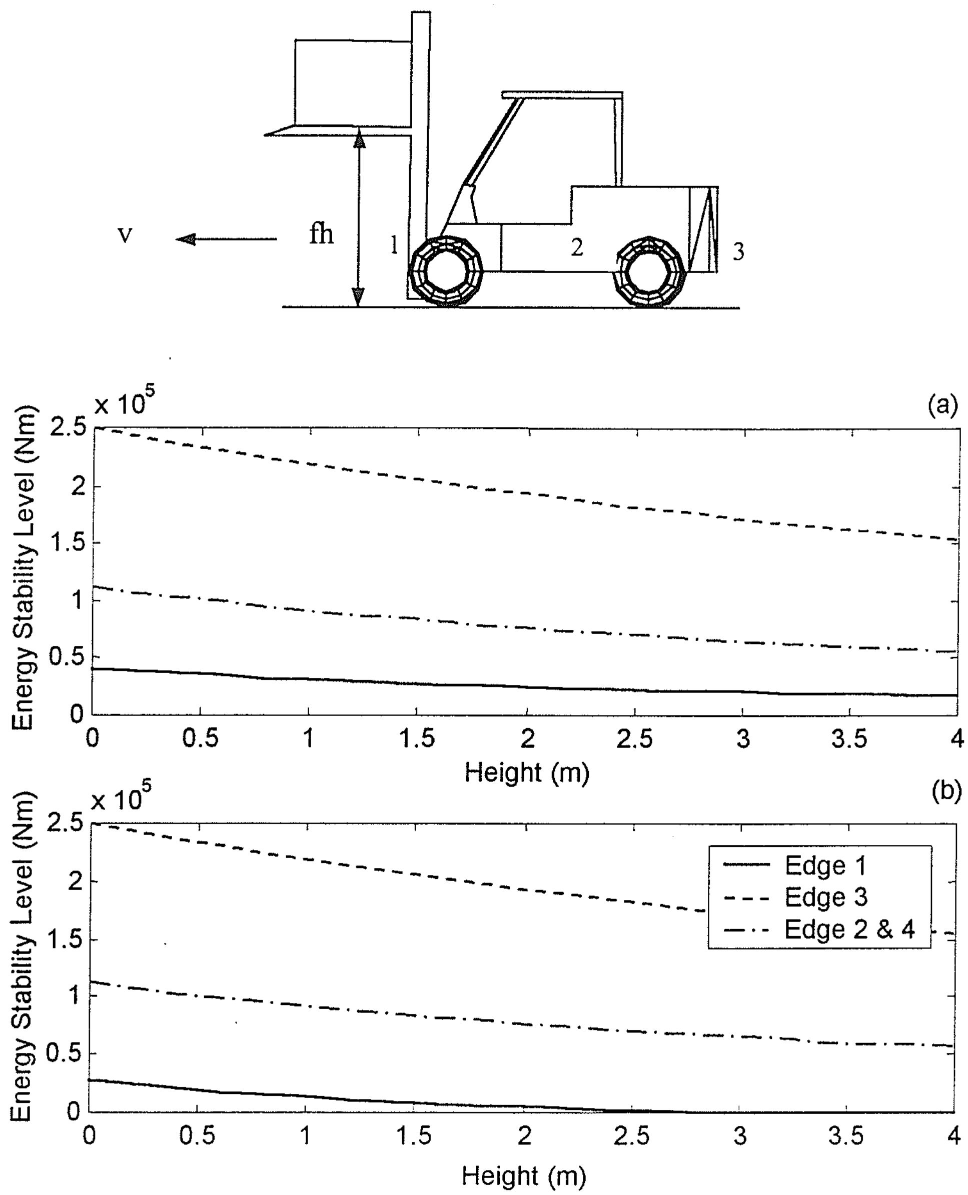

Figure 4.10: Effect of fork height on the stability of forklift:

(a) Constant velocity; (b) Abrupt stop.

4.2.4 Size of Wheelbase

The effect of wheelbase size on the stability level of each edge of the forklift is shown in Figure 4.11. It shows that with an increase in the wheelbase, the stability levels of edges 1 and 3 increases. Figure 4.11b shows that at the speed of 6 km/h, when the vehicle is brought to an abrupt stop, it is stable only if the wheelbase is more than 2.4 m. The actual wheelbase of a Caterpillar DP-90 forklift is 2.58 m. The decrease in stability level of edge 1 is 36% when the wheelbase of the vehicle is reduced to 2.50 m from 2.58 m. The increase in wheelbase from 2.58 m to 2.70 increases the energy stability level of the forklift by 56% for edge 1.

It is observed that the velocity has no effect on the stability level of edges 2, 3, and 4 as it is the same for sudden stop and constant velocity. Figure 4.11 also indicates that at a large wheelbase of the forklift, the effect of sudden stop on the stability of the forklift will be ineligible.

For the case of sudden stop (Figure 4.11b), it is seen that when the wheelbase of the vehicle increases from 2.58 m to 2.70 m, the load on the fork can increase by 400 kg. Further increase of 10 cm of the wheelbase, the load on the fork can increase by an additional 300 kg without affecting the stability on the forklift over edge 1.

4.2.5 Effect of Speed

The effect of speed (see Figure 4.12) on the stability of the forklift when it is brought to abrupt stop is discussed in this section. It is seen that as the speed of the vehicle is increased from –15 to 0 km/h, the stability level of edges 2, 3 and 4 increases. There is a decrease in the stability level of edge 1 as the speed of the vehicle is increased from 0 to 15 km/h (see Figure 4.12b). The vehicle becomes is subject to tipping over on edge 1 as the vehicle speed is increased from 7 km/h.

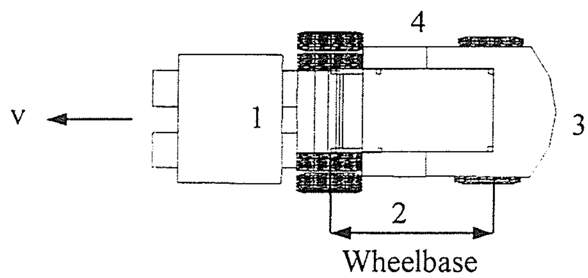

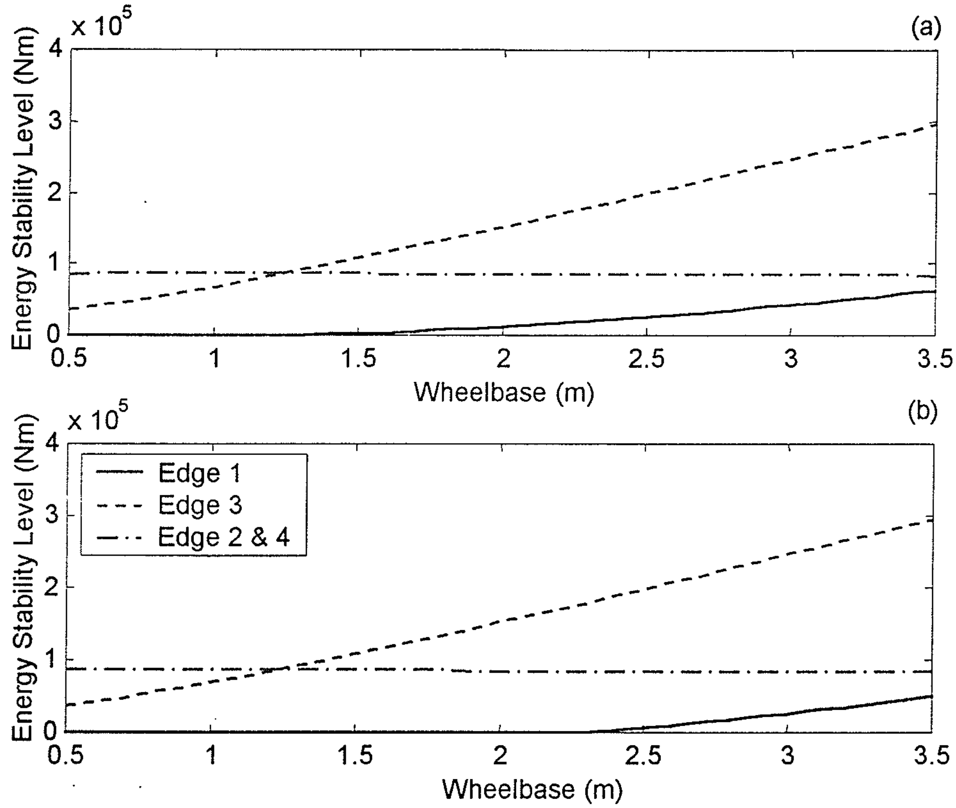

Figure 4.11: Effect of wheelbase on the stabilty of forklift:

(a) Constant velocity; (b) Abrupt stop.

There is a decrease of 94 % in the stability level of edge 1 as the vehicle speed is increased from 1 to 7 km/h. Comparing the results of various simulations, it is seen that if the speed of the vehicle is reduced from 7 km/h to 1 km/h, the load on the fork can be increased from 5,000 kg to 9,500 kg without affecting the stability of the forklift.

4.2.6 Effect of Variable Acceleration/Deceleration

This section investigates the effect of variable acceleration on the stability of the forklift. A six-degree polynomial equation is used to calculate the acceleration at a given time. The load on the fork is 5,000 kg and the forklift is moved a distance of 100 meters in 30 seconds. The results (see Figure 4.13) show that with an increase in acceleration the stability of edges 2, 3 and 4 decreases whereas the stability of edge 1 increases. As the vehicle decelerates to a constant velocity, the energy stability level of edge 1 is decreased with the increase in deceleration whereas the stability of the other edges increases with the deceleration. Figure 4.14 shows the close up of the energy stability level for edge 1.

4.2.7 Effect of Turning Angle

Figure 4.15 shows the effect of turning angle (θ_v) on the stability of the forklift. Figure 4.15a shows that for all the edges, the turning angle does not affect the stability of the forklift when it is moving at constant velocity. For the case of abrupt stop (see Figure 4.15b), the energy stability level of edge 1 increases with the increase in turning angle whereas there is the decrease in stability level of edge 2. With the increase in turning angle of the forklift from 0° to 45° there is an increase stability level by 9490 Nm, which is approximately 53% increase in the stability level. For edge 2, the increase in turning angle from 0° to 45°, the stability level of edge 2 decreases by 6070 Nm (see Figure 4.15b). Figure 4.16 shows the close up of the energy stability levels of edges 1 and 2.

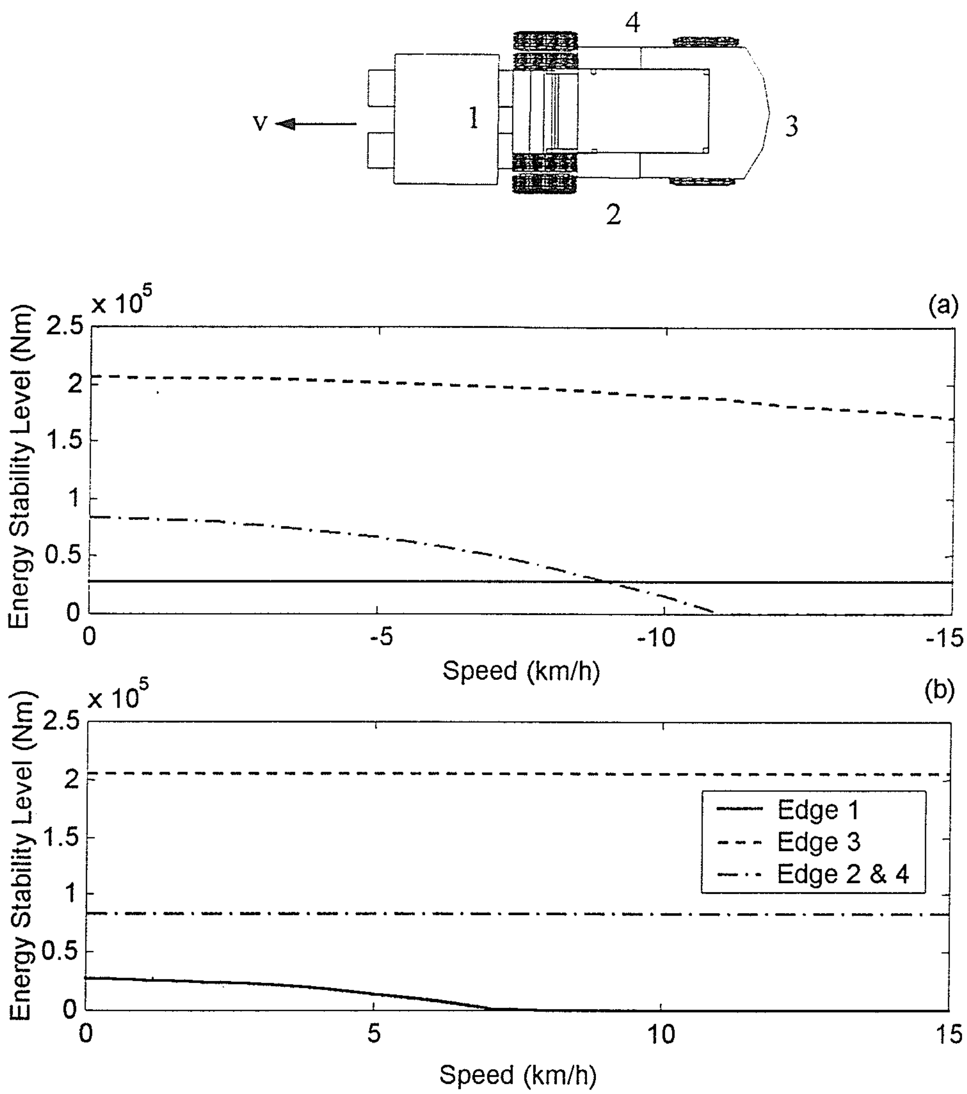

Figure 4.12: Effect of speed on stability of forklift at an abrupt stop.

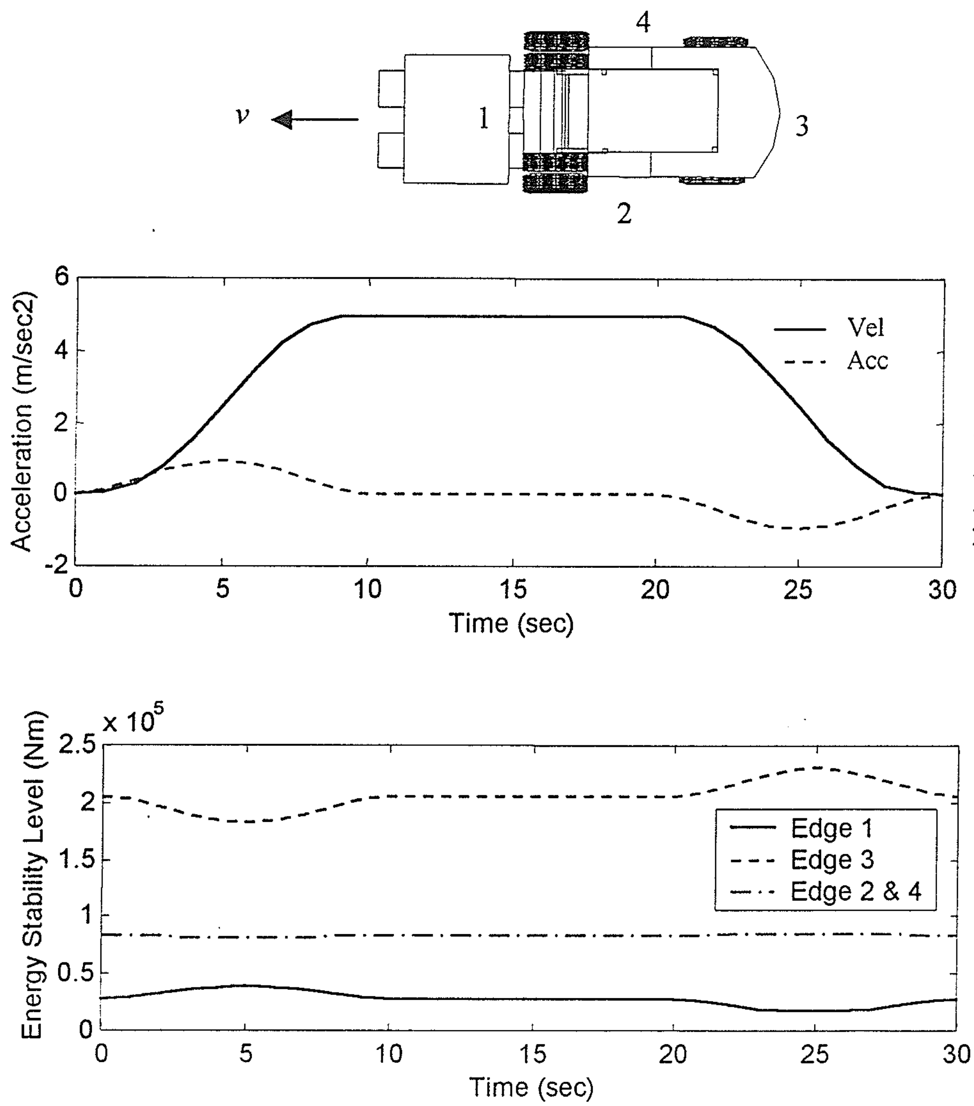

Figure 4.13: Effect of variable acceleration/deceleration on stability of forklift.

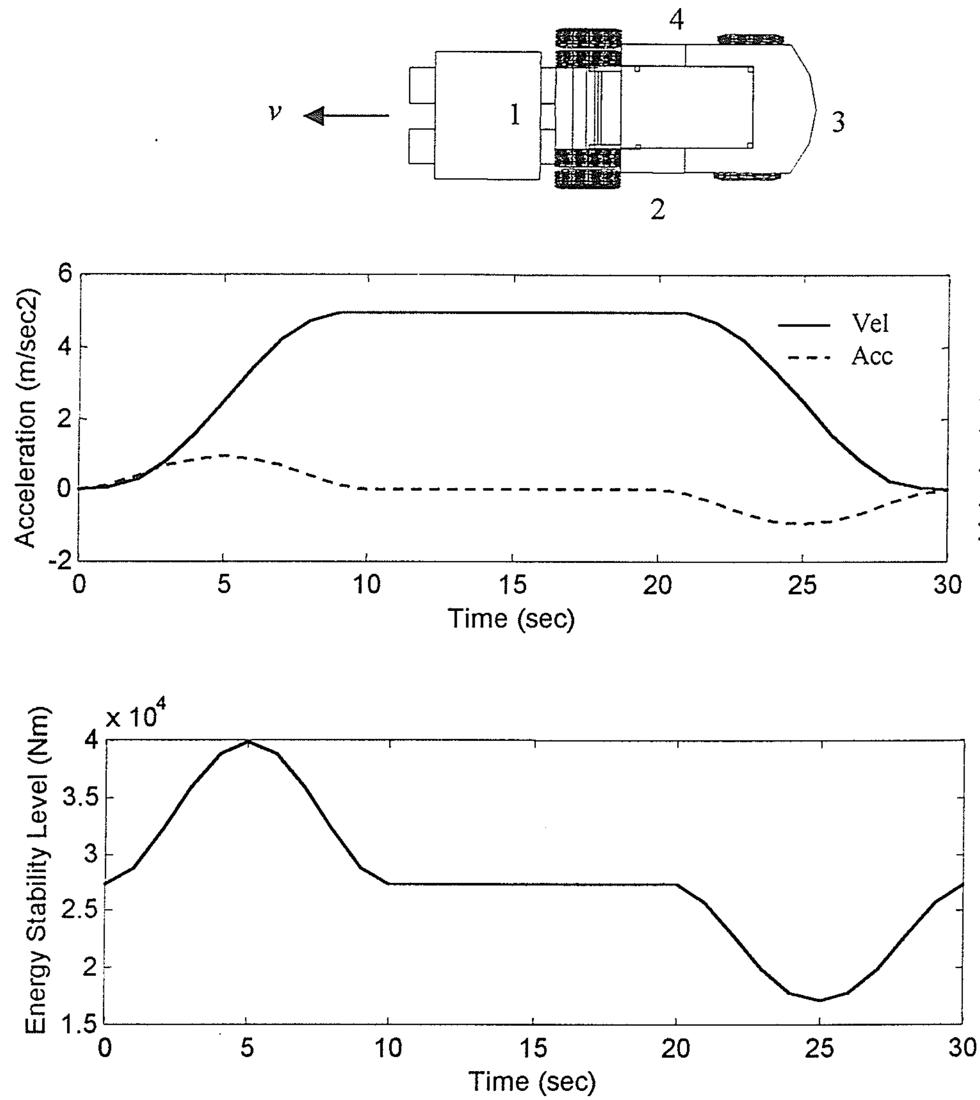

Figure 4.14: Effect of variable acceleration/deceleration on stability of edge 1.

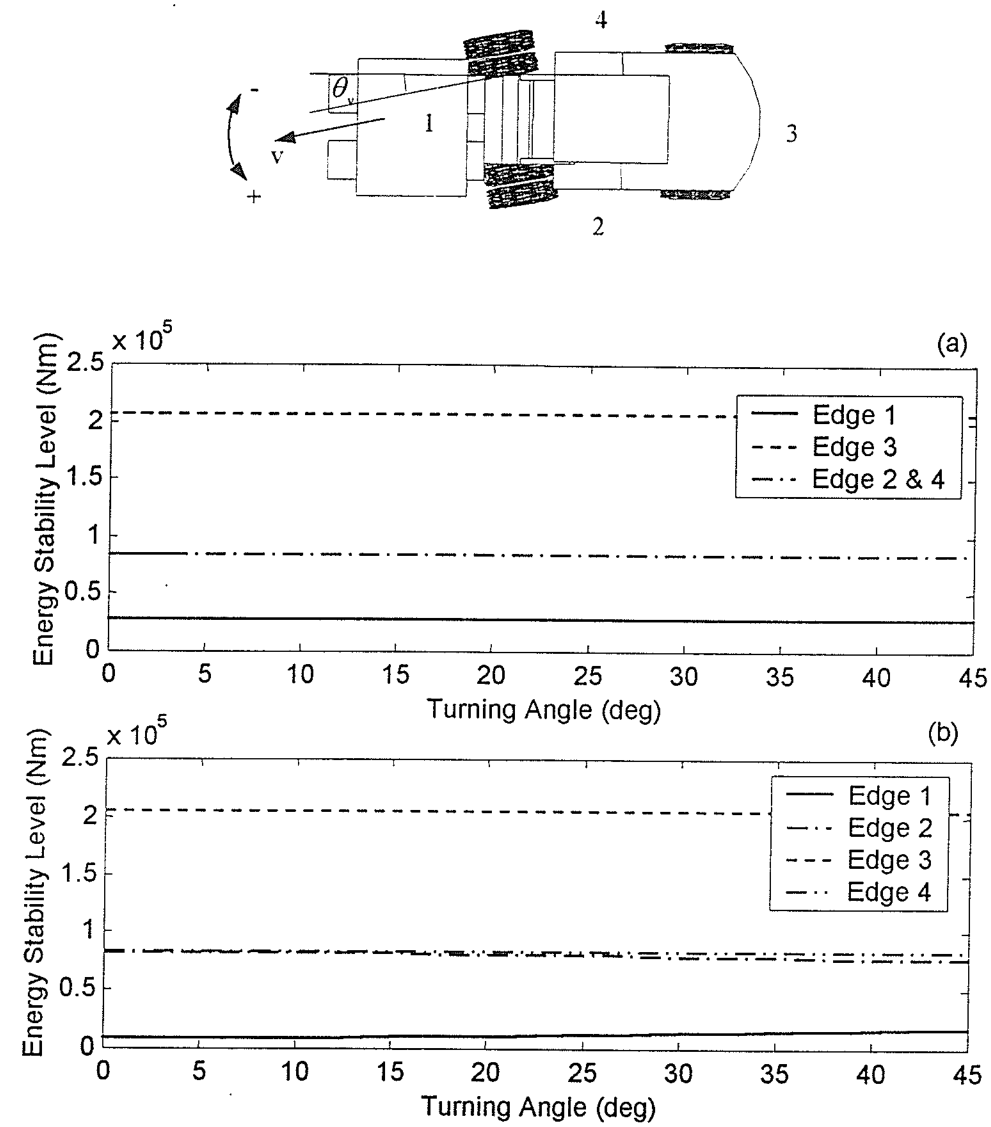

Figure 4.15: Effect of turning angle on the stability of forklift:
(a) Constant velocity; (b) Abrupt stop.

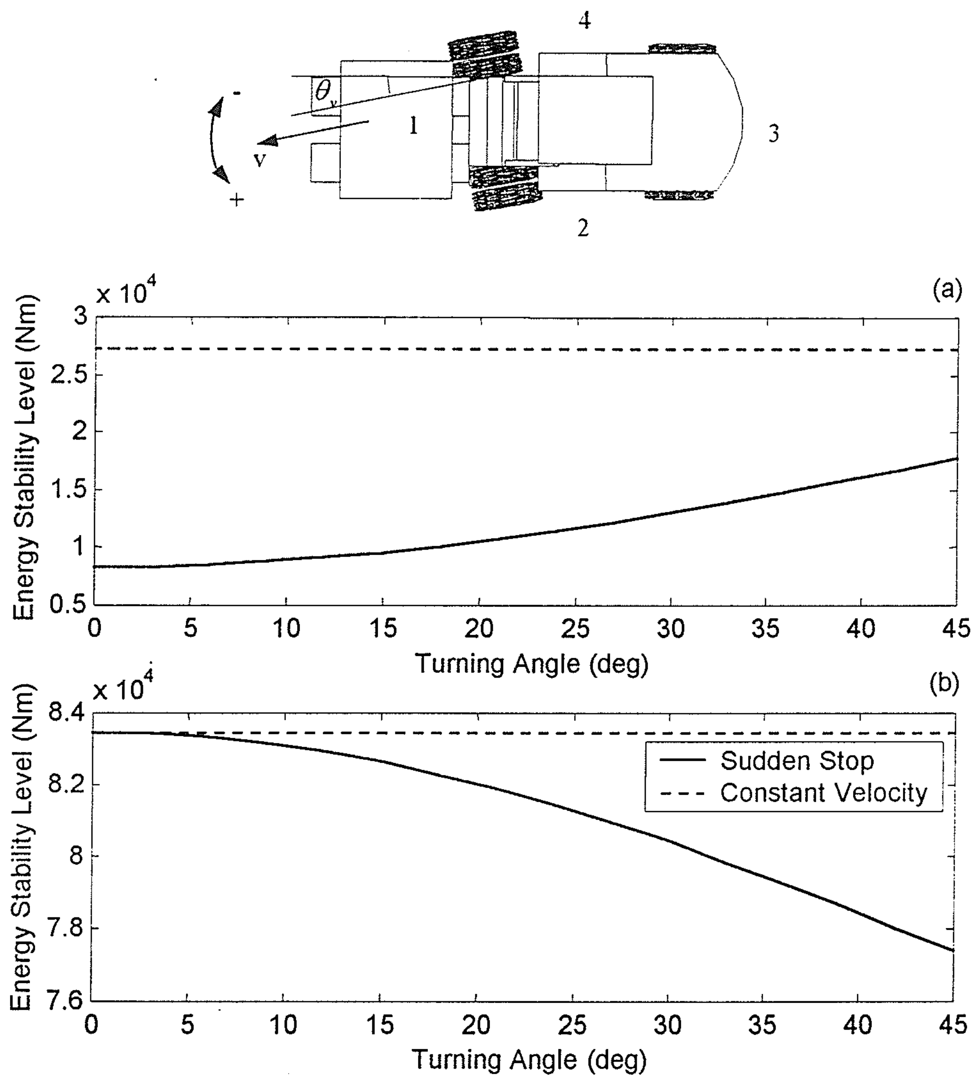

Figure 4.16: Effect of turning angle on the stability of edges 1 and 2:

(a) Edge 1; (b) Edge 2.

Chapter 5

Conclusions

According to the Occupational Safety and Health Act - OSHA, powered industrial equipment accounts for approximately 35,000 serious and 62,000 non-serious injuries each year. Approximately 100 of these accidents result in death. It costs the industry millions of dollars in damages incurred on products and equipment. OSHA has identified key factors that have contributed to employee accidents involved with lift trucks. Tip-overs account for approximately 25% of the all the forklift accidents. When forklifts are compared to an ordinary automobile, they have been found to be highly unstable.

The objective of this thesis was to develop a computer software to determine the potential tipping over of forklifts. The variables of instability such as load, top heaviness, speed etc were identified and their impact on the stability of forklifts was studied. First various methods that can be used to determine stability of forklifts were studied and discussed. Then the most suitable (energy stability concept) was chosen to develop the software. This concept was further extended to include the effects of acceleration and deceleration on the stability of the vehicle.

Visual C++ was the programming language used in developing this software application. Open GL was used to display the graphics. Open GL is independent of operating systems and hardware platforms, making it independent graphics library designed to be easily portable and rapidly executable.

The software developed was applied to Caterpillar DP-90 forklift and stability analysis was carried out. Results from this analysis are shown in this report. The results showed that at a load of 5,800 kg and the height of the fork is 1.5m, the forklift can tip over the front edge at 6 km/h, when the vehicle is brought to sudden stop. The maximum load recommended on this forklift is 9000kg. Further, it is observed that if the fork is moved from 1.6m to ground level the load on the fork can be increased from 5,000kg to 6,600 without jeopardizing the stability of forklift. It is observed that top heaviness is one of the key factors in the stability of forklifts.

These results can be used can be used as reference for further analyses. Designers can employ the results to improve the design of similar machines. This software can also be useful to put constraints on variables such as load and speed to ensure the safety of the operators and the machines. The effects of these variables can be easily compared, keeping one or more of the variables constant. This will provide a better understanding and grasp of stability of forklifts.

This study can be extended to include total or partial integration of this software with hardware – in this case with forklifts. The software part can analyze loads on all axles of forklifts and put an automated limit on acceleration and speed. This could ensure safety of the operator without much dexterity on his/her part, which comes with experience.

References

[1] Swartz, G., 1999, *Forklift Safety: A Practical Guide to Preventing Powered Industrial Truck Incidents and Injuries*, Government Institutes, Rockville Maryland.

[2] Lampi, H., " May the forces be with you: Pin down the principles influencing vertical RT forklift stability", www.liftlink.com

[3] Mcgee, R.B., and Frank, A.A., 1968, "On the Stability Properties of Creeping Gait", *Mathematical Biosciences*, Vol. 3, No. 2, pp. 331-351.

[4] Song, S.M., and Waldron, K.J., 1987, "An Analytical Approach for Gait Study and its Application on Wave Gaits", *The International Journal of Robotics Research*, Vol. 6, No. 2, pp 60-71.

[5] Messuri, D., and Klien, C.A., 1985,"Automatic Body Regulation for Maintaining Stability of a Legged Vehicle During Rough-Terrain Locomotion", *IEEE J. Robotics and Automation*, Vol. RA-1, No.3, pp 132-141.

[6] Ghasempoor, A., Sepehri, N., "A Measure of Stability for Mobile Manupulators With Application to Heavy-Duty Hydraulic Machines", *Journal of Dynamic Systems, Measurement, and Control*, Vol. 120, pp. 360- 370.

[7] Suggano, S., Huang, Q., and Kato, I.,1993 "Stability Criteria in Controlling Mobile Robotics System", *IEEE/RSJ International Conference of Intelligent Robots and Systems* , Yokohama, Japan, pp. 832-838.

[8] Leinecker, R., et al., 1999, *Visual C++ 6 Bible*, IDG Books Worldwide Inc., Chicago.

[9] Beer, F. P., and Johnston Jr., E.R., 1977, *Vector Mechanics for Engineers*, McGraw Hill Book Company, Toronto.

[10] Davidson, J. K., and Schweitzer, G., 1990, "A Mechanic-Based Computer Algorithm for Displaying the Margin of Static Stability in Four Legged Vehicles", *ASME Journal of Mechanical Design*, Vol. 112, pp. 480-487.

[12] Hunt, K. H., 1978, *Kinematic Geometry of Mechanisms*, Clarendon Press, Oxford.

[13] Graham, J.L., "Moving into balance: Specification perceptions on telescopic handlers", www.liftlink.com

[14] Graham, J.L., "Moving into balance: Specification perceptions on telescopic handlers", www.liftlink.com

[15] Nicklas, S., " The Geometry of Forklift Stability: Locking up Systems increase Forklift Stability, but Effective use Requires Thorough Understanding" , www.liftlinks.com

[16] Singh, N., 1996, *System Approach to Computer Integrated Design and Manufacturing*, John Wiley and Sons, Inc., New York.

Appendix A

Dimensions of Caterpillar DP-90 Forklift